UNIVERSITY OF LEEDS

SCHOOL OF EARTH AND ENVIRONMENT
University of Leeds
Woodhouse Lane
Leeds, LS2 9JT, UK
Tel: +44 (0)113 34 39086
E-mail: r.ivanovic@leeds.ac.uk
http://homepages.see.leeds.ac.uk/~earri
www.see.leeds.ac.uk/people/r.ivanovic

28th January 2014

Dear Yves Godderis,

Please find attached our revised paper. We found both reviewers' comments on the manuscript to be very helpful and have responded in detail below. In particular, throughout the changes and whenever possible we have tried to focus the paper on the most important aspects of our results, thus shortening the paper.

(The attached manuscript is in track-changes format for easy identification of the modifications made to the original manuscript. Please note that at Reviewer 2's request – see point 7 below – we have inserted a new Figure between previous Figure 2 and 3. We have tried to be clear in our response about the new Figure numbering. Text quoted from the manuscript is in italics.)

Reviewer 1

Reviewer's summary: 'The Messinian Salinity crisis is a very peculiar event in the Earth's history. It has been largely studied over the last 3 decades but how this multi-phase event impacted Late Miocene global climate remains to be studied. This paper attempts to clarify this question.

'This modelling exercise consists of the use of the fully coupled AOGCM HadCM3 to simulate the response of atmosphere (in term of air surface temperature mostly) and ocean (in term of surface temperature, potential temperature at depth, salinity, meridional overturning) to different scenarios combining the salinity of the Mediterranean Sea (from fresh water to hyper-saline water) and the intensity of the Meridional Outflow water (from a no-exchange to a twice stronger exchange). The paper is clear and well written.'

'However I think that some points need to be clarified.'

1. **Reviewer's comment:** 'The authors use a "Messinian control" as a reference simulate for that period. In this run, the model is forced with boundary conditions representing the Early Pliocene (EP) (PRISM2 dataset). It includes EP

topography, EP vegetation, reduced ice sheets and a pC02 fixed at 400 ppm. The authors give some references (Haywood and Valdes, 2004; Lunt et al., 2008a, 2008) in which the reader will find a full description of the simulated EP climate. However these papers did not give a full description of the simulated EP climate simulated with HadCM3. For instance, the air surface temperature shown in the paper (fig.4a [now figure 5a]) seems to be different from the figure 1 (top left) in Haywood and Valdes (2004). Concerning the two other papers (Lunt et al., 2008a and 2008b), they do not provide any further information how the AOGCM HadCM3 simulates the "Messinian" control (or Early Pliocene) at global scale since they consists mainly of sensitivity experiments to pCO2, topography, closure of seaway. I think that a more detailed description of the EP simulations will be useful. For instance, the authors should explain by how much the simulated EP climate is so warm, especially at low latitudes. The figure 4a [now figure 5a] does not permit to distinguish the respective effect of the rise of pCO2 (400 ppm vs 280 ppm), topography changes (fig.4d [now figure 5d]), and/or albedo changes. Changes in surface albedo can be shown. The sea surface temperature anomaly (fig.4b [now figure 5b]) should be discussed. The figure 4c [now figure 5c] (precipitation minus evaporation anomaly given in percentage) does not permit to observe the wetter and drier zones. These anomalies should not be explained in %. The authors must quantify the global mean difference in air surface temperature, precipitation, the change in NADW.'

Authors' response: The simulation run by Haywood and Valdes (2004) is an identical simulation to our *Miocene Control*, <u>except</u> that it has a closed Central American Seaway (CAS). This is why their figures (e.g. of surface air temperature) are different to ours. Lunt et al. (2008b) ran the same simulation to Haywood and Valdes (2004), <u>but with an open CAS</u>. This later simulation is completely identical to our *Miocene Control*. Because Lunt et al. (2008b) examined their simulation in the context of a closing CAS (when moving from the Miocene into the Pliocene), the anomalies are presented in this light. However, the differences are equally valid for looking at the effect of opening the CAS on the simulation described by Haywood and Valdes (2004). <u>We have modified the text in section 2.3.1 to clarify this point.</u> We have also removed references to Lunt et al. (2008a) here, because as the reviewer points out, it is not as relevant as Lunt et al. (2008b). Because Lunt et al. (2008b) do examine both the boundary conditions and the climate for our *Miocene control* in considerable detail with respect to Haywood and Valdes (2004) (albeit in the reverse context), we have not repeated this in the manuscript; the information presented would not be new and would lengthen the article considerably. However, we agree with the reviewers that not enough information was previously given and so <u>have extended the text in section 2.3.1 of the original manuscript to include more description of the control climate</u> e.g. global mean differences in air surface temperature, sea surface temperatures, precipitation and NADW formation. In agreement with the reviewer, <u>we have also changed Figure 5c (previously Figure 4c) to show precipitation (% change)</u>, which provides more useful information on the control climate.

2. **Reviewer's comment:** 'The sensitivity experiments to changes in MOW exchange and Mediterranean salinity are interesting. The authors have selected the three most pertinent experiments. However the authors must better explain how the "most pertinent" simulations were selected. In the discussion, they indicate that the chosen simulations can't be associated with a peculiar stage of the Messinian Salinity crisis. Thus the choice of the runs is not clear. The full data can not be accessed on the website.'

   Authors' response: <u>We have extended the text to include this explanation</u>; please also see our response to points 11 and 15 below. The full data can currently be accessed on the website by requesting a username/password from Paul Valdes. It will all be added to the open-access 'Simulations featured in papers' part of the website upon publication of this manuscript; you will see examples of the data for the other published papers on this theme are available in this way: http://www.paleo.bris.ac.uk/ummodel/scripts/papers/main_table1.html

3. **Reviewer's comment:** 'I suggest that the authors should discuss the role of salinity changes and MOW exchanges separately.'

   Authors' response: There are three reasons why we have not done this:
   1) A previous paper does this for the modern, pre-industrial HadCM3 set-up in some detail (Ivanovic et al., in press) and we do not think that there would be much additional gain from re-examining these questions independently.
   2) Whilst idealised, the changes we have tried to represent are changes in the direction we expect to have taken place during the Messinian Salinity Crisis (i.e. a reduction in Gibraltar Straits' geometry, crudely parameterised by the HadCM3 Mediterranean-Atlantic 'pipe' exchange coefficient, is highly likely to have occurred during Mediterranean hypersalinity, with the greatest reduction taking place during halite saturation), so it is useful to consider these processes together and relative to each other.
   3) Changing the coefficient of Mediterranean-Atlantic exchange in our simulations did not seem to affect the modelled processes; only the magnitude of the changes was affected for each set of salinity experiments, with the largest magnitude of change taking place when the exchange was greatest and vice versa.
   Also considering the editor's comments regarding conciseness, we think this is the most appropriate and informative way to present the results.

4. **Reviewer's comment:** 'The figure 8 [now figure 9] displays the impact on annual mean surface air temperatures but it would be interesting to display the changes in sea ice and/or surface albedo. A seasonal approach may be useful. Moreover the authors should add a sentence about possible feedbacks due to vegetation changes.'

   Authors' response: In response to later comments and the Editor's advice, we have refocused the manuscript to concentrate on the 'ample responses' to ‘shorten the paper’. In order to do this, we have removed discussion of sea-ice effects and seasonality. This is partly because we realised our presentation of the sea-ice results was not clear in the original manuscript. Our references to ‘sea-ice formation’ and ‘sea-ice cover’ are in fact descriptions of the change in sea-ice concentration, which is a confusing concept. This also explains why we described relatively large changes in sea-ice cover as a response to relatively small and localised temperature anomalies (see Editor’s comment). Because it is of secondary importance to the climate anomalies simulated, we have removed discussion of it from the manuscript.

The experiments were not run with a dynamic vegetation model so there are no simulated feedbacks (we have clarified this by extending the model description in section 2.1). It is beyond the scope of this study to investigate the vegetation response.

5. **Reviewer’s comment:** ‘In the last part of the discussion, the authors concluded that air temperature is very sensitive to MSC. However the impact on precipitation is not shown and/or discussed. Finally the authors suggest that regions can be defined as key zones. It is not so obvious according to figure 8 [now figure 9].’

   Authors’ response: The impact on precipitation is negligible in the hypersaline simulations and localised in the hyposaline simulations (as outlined at the end of section 3.2.2 and briefly discussed in the fourth paragraph of section 4). In agreement with the second reviewer and the editor, we have focussed the discussion on the ‘ample responses’ and so have not extended the text or figures further; precipitation is not majorly affected by the changes in MOW.

   With regard to the reviewer’s comments on Figure 9 (previously Figure 8); we have modified the figure to focus on the regions with the most ample responses (e.g. see our reply to point 20 below). In response to this modification and this comment by Reviewer 1, we have modified this text (i.e. the last two paragraphs of section 4 ‘Discussion and conclusions’) so that it is more appropriate.

6. **Reviewer’s comment:** ‘The red shades used in the colour scales of different plots (figures 4a, 4b, 8a [now figures 5a, 5b and 9a] etc) are hard to distinguish.’

   Authors’ response: We have deferred to the editor’s guidance that the colour scales do not need to be changed.

Reviewer 2

Reviewer’s summary: ‘In this paper, Ivanovic et al. use the HadCM3 model to test the impact of the MOW on the global ocean circulation and on the global climate. Starting from a Pliocene experiment, the authors modulate the exchange flux between the Mediterranean Sea and the Atlantic Ocean by imposing the global salinity of the Mediterranean Sea. The idea is to mimic the effect of highly saline and highly fresh Mediterranean water flowing into the Atlantic Ocean. The paper is generally well written but with too much details being unsupported by clear illustrations. The authors try to go deep into the details for explaining the response of their model but it is often hard to follow. The effect of the MOW remains weak in HadCM3 despite the efforts of the authors to find a well distinguishable signal in their runs. I have several comments listed below that require a substantial work from the authors before this paper could reach the standards of the journal. I think that this paper will be better in a shorter format and that, as it stands, it is too long, with too many details to provide explanations on very small signals.'

7. **Reviewer's comment:** 'P. 4813, please provide a figure - with a focus on the Gibraltar straits - with the ocean grid resolution - in order the reader can understand which ocean grid points are concerned by the equation (1). Indeed, you are referring to 4 points for the mean of each tracer field but it is not clear where they are located.'

   Authors' response: <u>We have added such a figure</u>, now Figure 3.

   Reviewer's comment continued: '…Also, why are you using a pipe of 1 km whereas today, the Gibraltar strait reaches 300 meters? Are there geological evidences? Please expand the discussion here.'

   Authors' response: The geological evidence that we use to ascertain that '*…1 km depth…is an appropriate palaeobathymetry in the model for either side of the Messinian Mediterranean-Atlantic seaways*' (page 4813 of the original manuscript) is cited in the text '(e.g. van Assen et al., 2006; Fortuin and Krijgsman, 2003; Hilgen et al., 2000; Hodell et al., 1994; Krijgsman, 2001; Krijgsman et al., 2004; van der Laan et al., 2006)' (page 4813 of the original manuscript). Because of the limits of the model's horizontal resolution, and to make sure that Mediterranean and Atlantic water flow out of the Straits and mix appropriately in the Gulf of Cadiz (Atlantic side) and Alboran Sea (Mediterranean side), the pipe must therefore also be this deep (otherwise a too-shallow pipe would extend too far in both directions). Furthermore, the pipe needs to be 1 km deep because it also necessarily captures part of the mixing of water masses that occurs above the continental shelf (which the model could not otherwise resolve properly). <u>We have extended the text before equation 1</u> to clarify this point.

8. **Reviewer's comment:** 'P. 4814, Figure 3 [now Figure 4] is described. Miocene and CTRL simulations are used to show salinity and temperature anomalies. I have an issue here, what are the boundary conditions used? What makes Miocene different than the CTRL?'

   'P.4815, Additional information about the boundary conditions (CO_2, CH_4, orbital parameters, solar luminosity) should be added here. Perhaps this information can be found in Lunt et al. (2008) but it is so fundamental for our understanding that it should be included here. ! The informations are on the next page in fact, l.16-20, perhaps, you could move these sentences on the previous page. !'

Authors' response: We have restructured these sections of the text so that the Miocene and modern control simulations (including Fig. 6., preciously Fig. 3) are now described after the boundary conditions are described, which we agree is a more appropriate order than was in the original manuscript. We have made the change this way around because we prefer to keep the description of the model's fundamental Mediterranean-Atlantic exchange equation before the description of the boundary conditions. (Note that this affects the numbering of several figures, which are now in a new order; specifically Fig. 4, 5 and 6 in the new manuscript). The description of the boundary conditions has also been moved up into the opening paragraphs of section 2.3.1, as suggested by Reviewer 2. The new order is: (1) a description of the Messinian model boundary conditions, (2) a general description of the Messinian model climate, (3) a description of Messinian model's Mediterranean-Atlantic exchange and Mediterranean Outflow Water. We have also extended the text in section 2.3.1 to provide a clearer description of the boundary conditions and a better description of the *Messinian control* climate. We have, however, kept these descriptions succinct as they are addressed in detail by two earlier publications; Haywood and Valdes (2004) and Lunt et al. (2008).

9. **Reviewer's comment:** 'P. 4816, what is the change in the land area induced by a 25 m higher sea level? Is it significant given the spatial resolution of the model?'

   Authors' response: As the reviewer suggests, the change in sea level (from present to Miocene) does not make a difference to the model's land-sea mask, however it does add an extra 25 m to the bathymetry and so is potentially significant.

10. **Reviewer's comment:** 'P. 4818. l. 11-13, even if the method is described in your previews paper, can you say some worlds in this paper in order the reader can follow what you did without being forced to read all your previous contributions.'

    Authors' response: We have extended the text here to clarify our methods. We also note that the reference to a previous paper is mainly made to highlight the consistency of the two investigations without having to read the detail of both methodologies. The reader is not required to also read the methods of the earlier paper; all necessary information is provided here.

11. **Reviewer's comment:** 'P.4818, Table1, what are the reasons that led to the choice of the values used for the coefficient of exchange. Why a quarter, than a half and then a doubling. It seems that this may be due to the decrease of the depth of the Gibraltar Strait, more saline water being equivalent to less water in the Mediterranean basin. Am I right? Please write it more explicitly in the paper.'

Authors' response: We have extended the text in the first paragraph of section 2.2 to clarify this. During the Messinian, the Gibraltar Straits were closed and Mediterranean and Atlantic were linked by two marine corridors; the Rifian Corridor through Morocco and the Betic Corridor through southern Spain (e.g. Betzler et al., 2006; Duggen et al., 2003; Martín et al., 2009; Santisteban and Taberner, 1983). The model would not resolve these gateways, and so the same parameterisation is used as for the Gibraltar Straits in the modern simulation to capture Mediterranean-Atlantic exchange. Part of the function of the coefficient of exchange in the parameterisation is to represent the geometry of the marine gateway(s) linking the two basins.

The MSC was likely brought about by changes in Mediterranean-Atlantic exchange volume (through either or both of the two Corridors), probably caused by regional tectonics and possibly also influenced by orbitally-controlled (mainly precession) climate. Whilst we do not yet know the exact nature of these changes (i.e. what were the dimensions of the Corridors and what were the exchange fluxes of water/salinity between the Mediterranean and Atlantic), it is highly likely that Mediterranean-Atlantic exchange was volumetrically reduced during episodes of hypersalinity. We do not know how it would have been different during episodes of hyposalinity.

Because of the uncertainty on the precise numbers (and even on Mediterranean Sea level at the time; e.g. Canals et al., 2006; Hsu et al., 1973; Roveri et al., 2011; Ryan and Cita, 1978), we chose to carry out idealised simulations in the direction of change that researchers think happened (based on both geological evidence and box modelling; e.g. Flecker and Ellam, 2006; Fortuin and Krijgsman, 2003; Krijgsman and Meijer, 2008; Lugli et al., 2010; Meijer, 2012; Topper et al., 2011). This included a halving and quartering of the exchange coefficient for the extremely hypersaline scenarios, where halite-saturation is thought to have occurred under conditions with the most restricted gateways. We do not know the direction of change that occurred during Mediterranean near-freshening, so we also halved and doubled the exchange coefficient for these simulations. However, because of the uncertainty in the direction of change, we focussed the analysis on the 1 x exchange coefficient simulation, rather than the halved or doubled scenarios. We have extended the text to make the justification clearer.

12. **Reviewer's comment:** 'P.4820, l.2-9, how do you follow a water mass in a eulerian OGCM? It is not clear to me. Can you expand the discussion here and/or provide convincing figure?.'

Authors' response: Here we are summarising the results described by a previous paper (Ivanovic et al., in press). In this paper, dye-tracers were used to directly track the path of Mediterranean-origin waters (Ivanovic et al., in press, p.7 and fig. 4). Notably, the use of dye-tracers in this study verified that temperature and salinity anomalies can also be used reliably to view the MOW plume in ambient Atlantic water in HadCM3 (e.g. Fig. 4, previously Fig. 3, of this manuscript), as they are in present-day observational profiles (e.g. Boyer et al., 2009). We have extended the text to make this paragraph clearer.

13. **Reviewer's comment:** 'P. 4820-4821 / l.26-6. This paragraph is hard to follow. The link between the NADW and the AABW is new for me and not straightforward, I am more used to seesaw in OAGCM, i.e. less NADW produces more AABW. Here the authors suggest a mechanism by which the decrease in NADW will produce the inverse. This is not convincing at all, please remove or expand. In addition, in the last sentence is wrong. Indeed, Fig. 5b [now Fig 6b] show the meridional overturning in the Atlantic Ocean (AMOC). The authors refer to the Pacific Ocean. Please be careful.'

    Authors' response: Following Reviewer 2's comments 13, 14, 18-21 and the Editor's guidance to 'focus your discussion on explaining the ample responses of the model to the sensitivity tests, without spending to [sic] much time on marginal responses', we have removed this paragraph. <u>We have edited the text to focus on the larger Northern Hemisphere changes and have removed discussion of the small Southern Hemisphere changes for the hypersaline simulations and other secondary processes for all simulations</u>. To be consistent, we have also <u>re-plotted some of the figures</u> to focus on the area of interest (around the North Atlantic). This includes figure 6 (previously figure 5), which depicts Atlantic Meridional Stream Functions for the different simulations, which were difficult to understand given that the Miocene North Atlantic was not an enclosed basin and had open water exchange with the Pacific through the Central American Seaway (hence invalidating the stream function plot across this latitude). <u>The text has been edited to accommodate this change.</u>

14. **Reviewer's comment:** 'The following paragraphs are also hard to follow. Again the authors describe many processes being causally linked but not always easy to follow. In particular they may at least change the figure 6 [now figure 7] by zooming on the area of interest where there is oceanographic signal in their runs, the Central and the North Atlantic.'

    Authors' response: In section 3.1, <u>we have amended figure 7 (previously figure 6)</u> as guided, have <u>removed text</u> that the reviewer and editor suggest is unnecessary (see response to point 13 above), and have <u>reworded parts of the text to make the explanation of the dominant processes clearer</u>.

15. **Reviewer's comment:** 'P.4822 l6-21. Concerning the salinity events, I would say that it would be more pertinent to compare the results from the simulations with the same exchange flux because here you change two factors, the salinity and the exchange flux. Otherwise, the authors could calculate the salinity exchange flux for each simulation and use these values to choose their run or to make their case more convincing. In fact, they do that in the next paragraph. So, provide us with salt export for each run shown in Table1.'

Authors' response: (Please also see response to point 3.) We have included the additional information in the table as requested and extended the text (also in response to point 2) to make our meaning clearer. Please note that we have not constrained the salinity exported from the Mediterranean, but allowed the GCM freedom to simulate this based on Mediterranean-Atlantic marine gateway(s) constraints. We controlled *μ* (e.g. halving, doubling etc.), which represents the geometry of the gateway(s) in the model (see response to points 2 and 11). We would also like to highlight that in terms of the processes discussed, there was little difference in the results depending on exchange-flux; '*the climate anomalies had the same direction of change and were brought about through the same mechanisms, although the magnitude of change was different depending on the exchange strength (varied μ, see Table 1); reducing the exchange damped the anomalies, enhancing the exchange exaggerated the anomalies*' (first paragraph of section 3.2). Although there were differences in the magnitudes of change when different exchange coefficients (*μ*) were used, we do not think this adds to the discussion of the results. This is especially true because (i) it would risk being repetitive of a previous paper that this work builds on (Ivanovic et al., in press); and (ii) it would increase the length of this manuscript, against the Editor's wishes, but would not greatly improve our understanding of either the mechanisms, or of the actual events because changes in gateway geometry almost certainly accompanied the salinity 'crises' (as previously discussed).

16. **Reviewer's comment:** 'P.4823 l1-2, can you explain the cooling induced by the salt export? 2 and 1.8 _C?'

    Authors' response: The cooling is caused by reduced vertical mixing. The reduced vertical mixing arises because at every timestep we have forced the Mediterranean to have uniform salinity throughout the water column. We have extended the text to include this explanation and clarify that it is not because of the salt export.

17. **Reviewer's comment:** 'L3-8, I do not see a more predominantly spreading of the MOW southward on figure 7 [now figure 8]. How can you state that the MOW is entrained in the ACC? Once again, I do not think that it is so easy to follow water path in an OAGCM.'

    Authors' response: We disagree; the positive salinity anomalies in Fig 8a and particularly 7b show that MOW mainly spreads south from the Gibraltar Straits (~35° N) and at depth, though this does not preclude some northward spread of MOW as well (especially Fig. 8a); we have extended the text to clarify this. With regard to entrainment in the ACC; we recognised temperature/salinity anomaly patterns (interpreted with respect to ocean currents) from similar, previously run experiments that contained dye-tracers (and so could track MOW directly). We are confident that this is what happens, however, because Reviewer 2 is not, we have removed the offending statement.

18. **Reviewer's comment:** 'L15 – l4(next page) / this paragraph is hard to follow, please remove it or rewrite it with a better choice of figure to support your logic.'

    Authors' response: <u>We have removed much of this (and the following) paragraph and rephrased what remains</u> so that it more clearly and succinctly describes only the key changes (also in response to points 13 and 14 above).

19. **Reviewer's comment:** 'P. 4824. L. 5-15 / The mid to high latitude SATs decrease by up to 4_C . . . in reality, I see a pattern closer to -0.5 to -1. Please avoid overstatement.'

    Authors' response: The figure quoted is accurate, there was cooling by '*up to 4 °C*'. However, we recognise that most (in fact almost all) of the cooling is less than this; a few degrees at most. <u>We have modified the text</u> to give an improved representation of the data. Note that <u>we have also modified the figure</u> to concentrate on the Northern Hemisphere region of most interest and not be distracted by 'very small signals' (see Reviewer 2's summary, above). This is in line with Reviewer 2 and the Editor's wishes to focus our presentation of the results (see response to points 13, 14, 18, 20 and 21).

20. **Reviewer's comment:** 'L16-24 / the SAT increase of 1.5 _C (fig. 8c [now fig. 9c]) is almost invisible . . . once again, your figure are not supporting your text.'

    Authors' response: <u>We have replotted the Figure 9 (previously Figure 8) panels</u> so that they are zoomed-in and the reader can see the climate anomalies of most interest (i.e. in the North Atlantic region) more clearly; including this localised 1.5 °C warming. Please also see previous responses, e.g. to points 13 and 19 above.

21. **Reviewer's comment:** 'L 25 – l12 (next page) lot of things are written here, once again very hard to follow, please remove or add diagnostics making your case more convincing. The elevated salinity (which is not visible) can explain both cooling and warming. The cooling is linked to more upwelling, the warming to a deeper mixed layer. All these explanations for changes in temperature of plus or minus 1_C . . .'

    Authors' response: <u>We have removed the text as suggested</u> (also see previous responses, e.g. to point 18 above).

22. **Reviewer's comment:** 'Figure 5 [now Figure 6] : A) it is strange, No intermediate waters goes south of 20 _N ? why that , the NADW should reach the southern hemisphere. Can you explain ?'

    Authors' response: The reviewer is right and deep/intermediate water does travel past the equator in the model; the problem is that the stream function plot is confusing (please see our response to point 13 above). The figure is difficult to understand in the Tropics because the Atlantic is not an enclosed basin here; the Central American Seaway is open. We realise that this rather invalidates the use of the stream function plot for this region, thus we have moved its cut-off north to 15° N (the Central American Seaway is just south of this) so that it now captures an enclosed segment of the North Atlantic basin.

Generally, we have revised the original manuscript so that it includes a better description of the model set-up and *control* climate. In addition, we have shortened the presentation and discussion of the results to remove reference to marginal effects and instead focus on the main climate responses (for this reason, we have removed rather than expanded the confusing presentation of small sea-ice changes, for example). We have also checked all of the numbers cited in the text (e.g. temperature changes) and where necessary, we have revised them to make sure that they are not overstated or focussed on extremes, but instead provide an accurate representation of the wider-spread effects. Several of the figures have been modified in line with the Reviewers' wishes; mainly to clarify and concentrate on the main processes/responses discussed in the text.

Therefore, having carefully and thoroughly addressed all of the reviewers' comments and responded to your guidance, we hope that the revised paper is now acceptable to be published in Climate of the Past.

Yours sincerely,

Ruža F. Ivanović

References cited

Van Assen, E., Kuiper, K. F., Barhoun, N., Krijgsman, W. and Sierro, F. J.: Messinian astrochronology of the Melilla Basin: Stepwise restriction of the Mediterranean-Atlantic connection through Morocco, Palaeogeography, Palaeoclimatology, Palaeoecology, 238(1-4), 15–31, doi:16/j.palaeo.2006.03.014, 2006.

Betzler, C., Braga, J. C., Martín, J. M., Sánchez-Almazo, I. M. and Lindhorst, S.: Closure of a seaway: stratigraphic record and facies (Guadix basin, Southern Spain), Int J Earth Sci (Geol Rundsch), 95(5), 903–910, doi:10.1007/s00531-006-0073-y, 2006.

Boyer, T. P., Antonov, J. I., Baranova, O. K., Garcia, H. E., Johnson, D. R., Locarnini, R. A., Mishonov, A. V., O'Brien, T. D., Seidov, D., Smolyar, I. V. and Zweng, M. M.: World Ocean Database 2009, NOAA Atlas NESDIS 66, edited by: Levitus, S., US Gov. Printing Office, Washington D.C., 216 pp., 2009.

Canals, M., Puig, P., Madron, X. D. de, Heussner, S., Palanques, A. and Fabres, J.: Flushing submarine canyons, Nature, 444(7117), 354–357, doi:10.1038/nature05271, 2006.

Duggen, S., Hoernle, K., van den Bogaard, P., Rüpke, L. and Phipps Morgan, J.: Deep roots of the Messinian salinity crisis, Nature, 422(6932), 602–606, doi:10.1038/nature01553, 2003.

Flecker, R. and Ellam, R. M.: Identifying Late Miocene episodes of connection and isolation in the Mediterranean-Paratethyan realm using Sr isotopes, Sedimentary Geology, 188-189, 189–203, doi:16/j.sedgeo.2006.03.005, 2006.

Fortuin, A. R. and Krijgsman, W.: The Messinian of the Nijar Basin (SE Spain): sedimentation, depositional environments and paleogeographic evolution, Sedimentary Geology, 160(1–3), 213–242, doi:10.1016/S0037-0738(02)00377-9, 2003.

Haywood, A. M. and Valdes, P. J.: Modelling Pliocene warmth: contribution of atmosphere, oceans and cryosphere, Earth and Planetary Science Letters, 218(3-4), 363–377, doi:16/S0012-821X(03)00685-X, 2004.

Hilgen, F. ., Bissoli, L., Iaccarino, S., Krijgsman, W., Meijer, R., Negri, A. and Villa, G.: Integrated stratigraphy and astrochronology of the Messinian GSSP at Oued Akrech (Atlantic Morocco), Earth and Planetary Science Letters, 182, 237–251, doi:10.1016/S0012-821X(00)00247-8, 2000.

Hodell, D. A., Benson, R. H., Kent, D. V., Boersma, A. and Bied, K. R.-E.: Magnetostratigraphic, biostratigraphic, and stable isotope stratigraphy of an Upper Miocene drill core from the Salé Briqueterie (northwestern Morocco): A high-resolution chronology for the Messinian stage, Paleoceanography, 9(6), PP. 835–855, doi:199410.1029/94PA01838, 1994.

Hsu, K. J., Ryan, W. B. F. and Cita, M. B.: Late Miocene Desiccation of the Mediterranean, Nature, 242(5395), 240–244, doi:10.1038/242240a0, 1973.

Ivanovic, R. F., Valdes, P. J., Gregoire, L., Flecker, R. and Gutjahr, M.: Sensitivity of modern climate to the presence, strength and salinity of Mediterranean-Atlantic exchange in a global general circulation model, Clim Dyn, 1–19, doi:10.1007/s00382-013-1680-5, in press.

Krijgsman, W.: Astrochronology for the Messinian Sorbas basin (SE Spain) and orbital (precessional) forcing for evaporite cyclicity, Sedimentary Geology, 140(1-2), 43–60, doi:10.1016/S0037-0738(00)00171-8, 2001.

Krijgsman, W., Gaboardi, S., Hilgen, F. j., Iaccarino, S., Kaenel, E. de and Laan, E. van der: Revised astrochronology for the Ain el Beida section (Atlantic Morocco): No glacio-eustatic control for the onset of the Messinian Salinity Crisis, Stratigraphy, 1, 87–101, 2004.

Krijgsman, W. and Meijer, P. T.: Depositional environments of the Mediterranean “Lower Evaporites” of the Messinian salinity crisis: Constraints from quantitative analyses, Marine Geology, 253(3–4), 73–81, doi:10.1016/j.margeo.2008.04.010, 2008.

Van der Laan, E., Snel, E., Kaenel, E. de, Hilgen, F. J. and Krijgsman, W.: No major deglaciation across the Miocene-Pliocene boundary: Integrated stratigraphy and astronomical tuning of the Loulja sections (Bou Regreg area, NW Morocco), Paleoceanography, 21, 27 PP., doi:200610.1029/2005PA001193, 2006.

Lugli, S., Manzi, V., Roveri, M. and Charlotte, S. B.: The Primary Lower Gypsum in the Mediterranean: A new facies interpretation for the first stage of the Messinian salinity crisis, Palaeogeography, Palaeoclimatology, Palaeoecology, 297(1), 83–99, doi:10.1016/j.palaeo.2010.07.017, 2010.

Lunt, D. J., Foster, G. L., Haywood, A. M. and Stone, E. J.: Late Pliocene Greenland glaciation controlled by a decline in atmospheric CO2 levels, Nature, 454(7208), 1102–1105, doi:10.1038/nature07223, 2008a.

Lunt, D. J., Valdes, P. J., Haywood, A. and Rutt, I. C.: Closure of the Panama Seaway during the Pliocene: implications for climate and Northern Hemisphere glaciation, Clim Dyn, 30(1), 1–18, doi:10.1007/s00382-007-0265-6, 2008b.

Martín, J. M., Braga, J. C., Aguirre, J. and Puga-Bernabéu, Á.: History and evolution of the North-Betic Strait (Prebetic Zone, Betic Cordillera): A narrow, early Tortonian, tidal-dominated, Atlantic–Mediterranean marine passage, Sedimentary Geology, 216(3–4), 80–90, 2009.

Meijer, P. T.: Hydraulic theory of sea straits applied to the onset of the Messinian Salinity Crisis, Marine Geology, 326–328, 131–139, doi:10.1016/j.margeo.2012.09.001, 2012.

Roveri, M., Bergamasco, A., Carniel, S., Gennari, R., Lugli, S. and Manzi, V.: The origin of Messinian canyons in the Mediterranean basin: towards an alternative model for the Messinian Salinity Crisis, oral presentation at the joint RCMNS-RCANS Interim Colloquium, Salamanca, Spain, 21–23 September, 2011.

Ryan, W. B. F. and Cita, M. B.: The nature and distribution of Messinian erosional surfaces — Indicators of a several-kilometer-deep Mediterranean in the Miocene, Marine Geology, 27(3–4), 193–230, doi:10.1016/0025-3227(78)90032-4, 1978.

Santisteban, C. and Taberner, C.: Shallow marine and continental conglomerates derived from coral reef complexes after desiccation of a deep marine basin: the Tortonian-Messinian deposits of the Fortuna Basin, SE Spain, Journal of the Geological Society, 140(3), 401–411, doi:10.1144/gsjgs.140.3.0401, 1983.

Topper, R. P. M., Flecker, R., Meijer, P. T. and Wortel, M. J. R.: A box model of the Late Miocene Mediterranean Sea: Implications from combined 87Sr/86Sr and salinity data, Paleoceanography, 26(3), PA3223, doi:10.1029/2010PA002063, 2011.

Modelling global-scale climate impacts of the late Miocene Messinian Salinity Crisis.

Ruza F. Ivanovic[1,2], Paul J. Valdes[2], Rachel Flecker[2] and Marcus Gutjahr[3]

[1]{School of Earth & Environment, University of Leeds, Leeds, United Kingdom}

[2]{School of Geographical Sciences, University of Bristol, Bristol, United Kingdom}

[3]{GEOMAR Helmholtz Centre for Ocean Research Kiel, Germany}

Correspondence to: Ruza F. Ivanovic (r.ivanovic@leeds.ac.uk)

Abstract

Late Miocene tectonic changes in Mediterranean-Atlantic connectivity and climatic changes caused Mediterranean salinity to fluctuate dramatically, including a ten-fold increase and near-freshening. Recent proxy- and model-based evidence suggests that at times during this *Messinian Salinity Crisis* (MSC, 5.96-5.33 Ma), highly-saline and highly-fresh Mediterranean water flowed into the North Atlantic Ocean, whilst at others, no Mediterranean Outflow Water (MOW) reached the Atlantic. By running extreme, sensitivity-type experiments with a fully-coupled ocean-atmosphere general circulation model, we investigate the potential of these various MSC MOW scenarios to impact global-scale climate.

The simulations suggest that although the effect remains relatively small, MOW had a greater influence on North Atlantic Ocean circulation and climate than it does today. We also find that depending on the presence, strength and salinity of MOW, the MSC could have been capable of cooling mid-high northern latitudes by a few degrees~~more than 1.2 °C~~, with the greatest cooling taking place in the Labrador, Greenland-Iceland-Norwegian and Barents Seas. With *hyper*saline-MOW, a component of North Atlantic Deep Water formation shifts to the Mediterranean, strengthening the Atlantic Meridional Overturning Circulation (AMOC) south of 35° N by ~~3~~1.5-6~~7~~ Sv. With *hypo*saline-MOW, AMOC completely shuts down, inducing a bipolar climate anomaly with strong cooling in the North (mainly -1 to -3 °C, but up to -~~10.5~~8 °C) and weaker warming in the South (up to +0.5 to +2.~~5~~ 7 °C).

These simulations identify key target regions and climate variables for future proxy-reconstructions to provide the best and most robust test cases for (a) assessing Messinian

model performance, (b) evaluating Mediterranean-Atlantic connectivity during the MSC and (c) establishing whether or not the MSC could ever have affected global-scale climate.

1 Introduction

During the latest Miocene (the *Messinian*) a series of dramatic, basin-wide salinity fluctuations affected the Mediterranean (Fig. 1). These are thought to have been caused by progressive tectonic restriction of the Mediterranean-Atlantic seaways (e.g. Hsu et al., 1977; Krijgsman et al., 1999a). This event, the *Messinian Salinity Crisis* (MSC), is recorded in a sequence comprising thick gypsum and halite evaporites (Fig. 1), which indicate a three to ten-fold increase in Mediterranean salinity above present day conditions (e.g. Decima and Wezel, 1973; Krijgsman et al., 1999a), and ostracod-rich *Lago Mare* facies, which suggest that at times, Mediterranean salinity declined to brackish or near-fresh conditions (Decima and Wezel, 1973).

The effect that the MSC may have had on global-scale climate has yet to be fully explored. Murphy et al. (2009) and Schneck et al. (2010) investigated the impact of Mediterranean Sea level change, as well as total evaporation and revegetation of the Mediterranean basin, using an atmosphere only General Circulation Model (GCM) and Earth system model of intermediate complexity, respectively. They found a generally localised impact (for example, 7 °C annual mean warming, ±600 mm yr^{-1} of precipitation, mostly in good agreement with the fossil-record; Griffin, 1999), mainly affecting the Alps and Northern Africa, but with some influence (cooling) over the high latitude oceans (North Atlantic, North Pacific and the Gulf of Alaska; Murphy et al., 2009). Others have considered the influence of Mediterranean Outflow Water (MOW) on present day and Quaternary global-scale climate through its ability to modify North Atlantic circulation (Bigg and Wadley, 2001; Chan and Motoi, 2003; Ivanovic et al., ~~in press~~2013c; Kahana, 2005; Rahmstorf, 1998; Rogerson et al., 2010). However, none have investigated the impact of MSC changes in MOW on ocean circulation and climate.

It has been widely postulated that there was no Mediterranean outflow during episodes of Mediterranean hypersalinity and this must have been true if the Mediterranean fully desiccated during halite precipitation (e.g. Hsu et al., 1973; Ryan and Cita, 1978). However, the evidence for complete desiccation remains controversial (e.g. Canals et al., 2006; Roveri et al., 2011) and alternative hypotheses have been put forward invoking a less substantial

Mediterranean sea level fall and even sustained MOW during periods of Mediterranean hypersalinity (e.g. Flecker and Ellam, 2006; Fortuin and Krijgsman, 2003; Krijgsman and Meijer, 2008; Lugli et al., 2010; Meijer, 2012; Topper et al., 2011). In addition, it is difficult to envisage how enough salt could have been brought into the Mediterranean to explain the 1-3 km thick Messinian evaporite sequence visible in the seismic record (Lofi et al., 2011; Ryan et al., 1973) without inflow from the Atlantic.

From box modelling and hydrologic budget calculations, total desiccation of the Mediterranean is estimated to have taken 1-10 kyr (Benson et al., 1991; Blanc, 2000; Hsu et al., 1973; Meijer and Krijgsman, 2005; Topper et al., 2011), producing a layer of evaporite that is 24-47 m thick in the process (Meijer and Krijgsman, 2005). This is less than 2 % of the total volume of evaporite thought to have precipitated out of solution in around 500 ka (Krijgsman et al., 1999a) or less (Garcia-Castellanos and Villaseñor, 2011) during the Messinian. Thus, one desiccation-reflooding cycle would be required approximately every 6-7 ka. The solar precession mechanism put forward to explain the observed cyclicity in Messinian Mediterranean sediments has a periodicity of 21 kyr (Krijgsman et al., 1999a); too long to reconcile the desiccation hypothesis with the volume of evaporites precipitated. Other hypotheses encompass cycles of 10 kyr or less (Garcia-Castellanos and Villaseñor, 2011).

A more likely scenario, consistent with both model results (e.g. Gladstone et al., 2007; Meijer and Krijgsman, 2005; Meijer, 2006, 2012) and data (Abouchami et al., 1999; Ivanovic et al., 2013a; Muiños et al., 2008) is that the Mediterranean was often connected to the Atlantic during MSC hyper- and hypo-salinity, particularly during episodes of gypsum formation and near-freshening, with at least periodic Mediterranean Outflow to the Atlantic.

It is the purpose of this modelling study to investigate both the impact of hyper- and hypo-saline MOW on global-scale Messinian climate and to evaluate the consequences of no Mediterranean water reaching the Atlantic. From this work, it is possible to determine the climate variables and geographical regions that are most susceptible to MSC-influenced climate changes. To this end, we here present a series of fully-coupled atmosphere-ocean GCM simulations, which assess Messinian climate sensitivity to extreme end-member changes in MOW that may have occurred during the MSC. In the absence of data to confirm whether or not MOW underwent dramatic fluctuations in salinity in the late Miocene, we ask the question of whether the MSC *could ever* have affected global-scale climate in the most extreme, geologically-constrained, Mediterranean salinity scenarios.

2 Methods

2.1 Model Description

The climate simulations for this study were run with the UK Met Office's fully coupled atmosphere-ocean GCM HadCM3, version 4.5. The atmosphere model has a horizontal resolution of 2.5° x 3.75°, 19 vertical layers (using the hybrid vertical coordinate scheme of Simmons and Burridge, 1981) and a timestep of 30 minutes. It includes physical parameterisations for the radiation scheme (as per Edwards and Slingo, 1996), convection scheme (as per Gregory et al., 1997) and land surface scheme (MOSES-1; Cox et al., 1999). This particular version of HadCM3 does not include a dynamic vegetation model; the vegetation distribution for each simulation is prescribed and remains fixed.

The ocean model is more finely resolved, with a 1.25° x 1.25° horizontal grid and 20 vertical levels that have been designed to give maximum resolution towards the ocean surface (Johns et al., 1997). It has a fixed lid, which means that the ocean grid boxes (and hence sea level) cannot vary. Consequently, evaporation, precipitation and river runoff are represented as a salt flux (Gordon et al., 2000). Included in the ocean model's physical parameterisations are an eddy-mixing scheme (Visbeck et al., 1997), an isopycnal diffusion scheme (Gent and Mcwilliams, 1990) and a simple thermodynamic sea-ice scheme of ice drift and leads (Cattle et al., 1995) and ice concentration (Hibler, 1979). Gordon et al. (2000) show that HadCM3 reproduces modern sea surface temperatures well without needing to apply unphysical 'flux adjustments' at the ocean-atmosphere interface.

The ocean equation of state is based on Bryan and Cox (1972) and is an approximation to the Knudsen formula (Fofonoff, 1962). Although this is a relatively old version, the percentage deviation from the UNESCO standards (Fofonoff and Millard, 1983) are small for salinities in the normal range (0-42 psu). At very high salinity values, none of the existing equations of state are valid. However, the density of sea water predicted from our approximation was within 1 % of those shown in Dvorkin et al. (2007) for the Dead Sea (at depth=0 and temperature=25 °C). Moreover, we are not attempting to predict the flow within the Mediterranean itself. Instead we are examining the effect of the outflow on the global climate system, and mxing close to the straights rapidly brings the hypersaline flow to within the validity bounds of the equation of state.

The ocean and atmosphere components are coupled once per model-day. To account for the different grid resolutions, the ocean grid is aligned with the atmosphere grid and thus the constituent models pass across the fluxes accumulated over the previous 24 model-hours by interpolating and averaging across the grids as appropriate. Rivers are discharged to the ocean by the instantaneous delivery of continental runoff (from precipitation) to the coasts, according to grid-defined river catchments and estuaries. Gordon et al. (2000) and Pope et al. (2000) give a more detailed description of the model and its components, including improvements on earlier versions.

With a new generation of high-resolution GCMs, HadCM3 may no longer be considered ‘state of the art’. However, its relatively fast model-speed (compared to more recent versions) enables long-integrations of several centuries to be made. This is necessary for ocean circulation to approach near steady-state in our simulations, so that the surface climates and large-scale ocean circulations and heat/salt transports, including Atlantic Meridional Ocean Circulation (AMOC), are in an equilibrium state in the model (Ivanovic et al., ~~in press~~2013c). Also, previous studies suggest that it is important to run the model for at least several centuries to capture the effect of changes in MOW on North Atlantic circulation and climate (Bigg and Wadley, 2001; Chan and Motoi, 2003; Kahana, 2005).

2.2 Mediterranean-Atlantic exchange

Neither the Gibraltar Straits (location indicated by Fig. 2), nor the late Miocene Mediterranean-Atlantic seaways (e.g. Betzler et al., 2006; Duggen et al., 2003; Martín et al., 2009; Santisteban and Taberner, 1983) can be resolved on the HadCM3 grid. Instead, a parameterisation of Mediterranean-Atlantic water exchange is employed for modern flow through the Gibraltar Straits, which partially mixes thermal and saline properties between the two basins based on temperature and salinity gradients and according to a constant coefficient of exchange (μ). As such, μ also represents the control of Mediterranean-Atlantic gateway geometry on the exchange. We have used the same parameterisation for the late Miocene simulations carried out in this study. Thus, the net heat and salt flux is calculated for two corresponding pairs of grid boxes, either side of the land-bridge linking the European and African continents (marked by the red crosses on Fig. 3). This is carried out in the upper 13 ocean levels of the model; 0 to 1 km depth, which is an appropriate palaeobathymetry in the model for either side of the Messinian Mediterranean-Atlantic seaways (e.g. van Assen et al., 2006; Fortuin and Krijgsman, 2003; Hilgen et al., 2000; Hodell et al., 1994; Krijgsman, 2001; Krijgsman et al., 2004; van der Laan et al., 2006)~~(e.g. van Assen et al., 2006; Fortuin and~~

~~Krijgsman, 2003; Hilgen et al., 2000; Hodell et al., 1994; Krijgsman et al., 2004; Krijgsman, 2001; van der Laan et al., 2006)~~. Although the continental seaways were probably not this deep, or at least not for the entire Messinian, because of the model's horizontal resolution constraints, the parameterisation also necessarily captures part of the mixing and flow that occurs above the continental shelf in the Gulf of Cadiz (Atlantic) and Alboran Sea (Mediterranean). If the *pipe* was shallower than this, flow through the marine gateways would reach too far into the Atlantic and Mediterranean basins at too shallow depth, and insufficient mixing bedtween Mediterranean and Atlantic waters would take place in proximity to the Straits. It is because of these model resolution limitations~~This is why~~ that a seemingly over-deep *pipe* is used to represent exchange through the seaway (similar to Ivanovic et al., ~~in press~~2013c). Thus, for every level and at every timestep, the mean of the four points is calculated for each tracer field ($\overline{T}$). Then, where T_j is the tracer for each of the four grid boxes, the difference between the old (previous timestep) and the new (current timestep) tracer is given as:

$$\left.\frac{\partial T_j}{\partial t}\right|_{pipe} = \mu(T_j - \overline{T}) \qquad (1)$$

(Gordon et al., 2000), where μ is a given coefficient of Mediterranean-Atlantic exchange and

$\left.\frac{\partial T_j}{\partial t}\right|_{pipe}$ is the tracer tendency for the *pipe* parameterisation.

This parameterisation (described in more detail by Ivanovic et al., ~~in press~~2013c) achieves ~1 Sv of easterly and westerly 'flow' through the Gibraltar Straits for the present day, which is close to contemporary observational values (>0.74 ±0.05 Sv; García-Lafuente et al., 2011). ~~For the Messinian model configuration, ~1.2 Sv of exchange is achieved due to the modelled westernmost Mediterranean being on average around 2 psu saltier than for the present day (with a volume integral of around 44 psu), and the easternmost North Atlantic being 1-2 psu fresher (with a volume integral of around 35 psu).~~ The model successfully simulates the two-layer flow structure observed for present-day exchange through the Straits (e.g. Bethoux and Gentili, 1999), with a surface eastward flow of North Atlantic Central Water (NACW) into the Mediterranean and a deeper westward flow of MOW into the Atlantic. Due to net evaporation over the Mediterranean, MOW is up to 2 psu saltier than the NACW it flows into (note that this difference is smaller than the difference in salinity between the westernmost Mediterranean and easternmost Atlantic due to mixing of the water masses in the exchange).

~~In the Miocene HadCM3 simulation (later referred to as *Messinian control*), MOW exports 1.2 psu Sv to the Atlantic. Consequently, a clearly distinguishable, relatively warm, high-salinity plume spreads westwards in the intermediate-deep North Atlantic (Fig. 3c and d). Such a relatively high-salinity plume is observed (e.g. Boyer et al., 2009) and modelled (e.g. Fig. 3a and b) in the modern ocean.~~

An important caveat to consider for this study is that the model is not fine-scaled enough to fully resolve the complex flow structure of MOW and Atlantic inflow water in ~~the~~ what is now the Gibraltar Straits-Gulf of Cadiz region (location indicated by Fig. 2). Consequently, Mediterranean eddies (*meddies*) and processes of North Atlantic entrainment in MOW are not directly simulated. *Meddies* are partially represented by μ in the Mediterranean-Atlantic exchange parameterisation, although overall, HadCM3 probably underestimates shallow-intermediate mixing of MOW with ambient NACW (Ivanovic et al., 2013b). North Atlantic entrainment, on the other hand, is represented by diffusive mixing of MOW with Atlantic water as it descends the continental shelf and spreads westwards. It is likely overestimated in HadCM3, because the model's depth-based (z) coordinate system (Johns et al., 1997, Table 2) incompletely resolves the dense, bottom-hugging overflow of MOW into the Atlantic (e.g. Griffies et al., 2000). These two effects partly counteract each other, resulting in the fairly good reproduction of the large-scale features of MOW in the North Atlantic today (e.g. as seen in Boyer et al., 2009). However, this also makes it difficult to interpret their individual impact on model sensitivity to changes in MOW buoyancy.

2.3 Experiment design

2.3.1 Messinian control configuration

The MSC took place at the end of the Miocene (5.96-5.33 Ma) and hence falls between the sub-epochs of the late Miocene (mid-point ~8 Ma) and early Pliocene (mid-point ~4.5 Ma). Key palaeogeographic characteristics of this period (Markwick, 2007) include lowered topography in the Americas and Himalayas, a reduced Greenland ice cap and an open Central American Seaway (CAS, location indicated by Fig. 2).

Compared to the modern set-up, the palaeo-configuration for the Messinian HadCM3 simulation (subsequently referred to as *Messinian control*) consists of raising global sea levels by 25 m, adjusting the topography to match Mio-Pliocene orography (Fig. 4d), reducing ice sheet size and height (-50 % for Greenland and -33 % for Antarctica, also visible in Fig. 4d) and implementing Pliocene vegetation distribution. We chose to use these palaeoenvironmental boundary conditions from the United States Geological Survey (USGS) Pliocene Research, Interpretation and Synoptic Mapping (PRISM) 2 ~~palaeoenvironmental boundary conditions~~project, as per Haywood and Valdes (2004), even though they were originally reported for the earlier period of 3.26-3.02 Ma (Dowsett and Cronin, 1990; Dowsett et al., 1999). ~~,~~ ~~but with an open CAS (370 m deep) as used by Lunt et al. (2008b).~~ This is because more recent work by the USGS (PRISM3) implies that the PRISM2 palaeoenvironmental conditions are closer to an early Pliocene configuration than a mid Pliocene one, particularly in terms of topography in the Americas and Himalayas (Haywood et al., 2010, 2011; Robinson et al., 2011).

~~In addition, r~~Recently presented neodymium isotope evidence (Dutay et al., 2012; Osborne et al., 2012) suggests that a shallow CAS remained open until around 3 Ma. Therefore, one change made to the model configuration of Haywood and Valdes (2004) was to open the CAS, as per Lunt et al. (2008).

Atmospheric CO_2 concentrations were set at 400 ppmv. Although this is at the high-end of (or exceeding) proxy-archive reconstructions from the Messinian (incl. Demicco et al., 2003; Pagani et al., 1999; van de Wal et al., 2011), considerable uncertainties over these reconstructions remain (Bradshaw et al., 2012). Also, using a lower-resolution ocean version of the HadCM3 GCM (HadCM3L), Bradshaw et al. (2012) show that a better match between Miocene model and proxy climate data is achieved using 400 ppmv compared with lower CO_2 concentrations.

In light of these current palaeoenvironmental findings, the PRISM2 *Pliocene* set up with an open CAS (370 m deep) and 400 ppmv level of atmospheric CO_2 would seem to capture the key ingredients of the late Miocene/early Pliocene world. Details of the PRISM2 *Pliocene* HadCM3 model set up and modifications to this configuration to include an open CAS are given by Haywood and Valdes (2004) and Lunt et al. (2008)~~(2008b)~~, respectively. (Note, that Lunt et al., 2008, present their findings in the chronological framework of the CAS closing through time. However, their results can also be viewed in the converse framework of opening the CAS relative to the results of Haywood and Valdes, 2004. This is the exact simulation that has been used as the *Miocene control* in this investigation, but *Miocene control* has been run for several millenia longer.)

The Messinian simulation was integrated for over 2,400 years to enable the ocean to reach near steady-state and provide the basis for all other simulations presented here. The *Messinian control* simulation is a 500-year continuation of this spin-up model run, with all other simulations also running for 500 years in parallel to this (reaching near-steady state within the first 400 years). In every case, the climate means were calculated from the final 100 years.

~~Detailed descriptions of the ocean circulation and climate simulated by the *Messinian control* are given by Haywood and Valdes (2004) and Lunt et al. (2008a, 2008b).~~ As outlined, the model set-up is identical to that used by Lunt et al. (2008), which is modified from Haywood and Valdes (2004), and thorough descriptions of the ocean circulation and climate simulated by the *Messinian control* are given by those authors. Briefly, in the late Miocene the world was warmer and wetter than it is today, although an overall cooling trend had set-in and the bio-climatic zones of the Messinian were much closer to present day than earlier Miocene conditions (e.g. Pound et al., 2012). With a global annual mean temperature of 16.7 °C, o~~O~~ur modelled Messinian world (*Messinian control*)~~, this study; Fig. 4a and b)~~ is ~~generally~~ ~ 3.4 °C warmer (Fig. 4a) and has +0.2 mm day^{-1} more rainfall (+73 mm yr^{-1}, both global annual means) than the equivalent modern~~, pre-industrial set-up~~ simulation, where the high latitude land masses and parts of the tropics are generally wetter, although some of the deserts and tropics have relatively less rainfall (Fig. 4c) ~~(from Ivanovic et al., in press)~~. ~~The high latitude land masses are also generally wetter, although some of the deserts and tropics get relatively drier (Fig. 4c). Compared to the modern set-up, the palaeo-configuration consists of raising global sea levels by 25 m, adjusting the topography to match Mio-Pliocene orography (Fig. 4d), reducing ice sheet size and height (-50 % for Greenland and -33 % for Antarctica, also visible in Fig. 4d) and implementing Pliocene vegetation distribution. Atmospheric~~ ~~CO_2 concentrations were set at 400 ppmv. Although this is at the high-end of (or exceeding) proxy-archive reconstructions from the Messinian (incl. Demicco et al., 2003; Pagani et al., 1999; van de Wal et al., 2011), considerable uncertainties over these reconstructions remain (Bradshaw et al., 2012). Also, using a lower-resolution ocean version of the HadCM3 GCM (HadCM3L), Bradshaw et al. (2012) show that a better match between model and proxy climate data is achieved using 400 ppmv compared with lower~~ ~~CO_2 concentrations.~~

In terms of ocean circulation, both proxy- and model-based research suggests that with an open CAS, Messinian North Atlantic Deep Water (NADW) formation would have been considerably weaker than for the present day (Böhme et al., 2008; Herold et al., 2012; Lunt et al., 2008; Molnar, 2008; Murdock et al., 1997; Prange and Schulz, 2004; Schneider and Schmittner, 2006; Steph et al., 2010; Zhang et al., 2012)~~(Böhme et al., 2008; Herold et al., 2012; Lunt et al., 2008b; Molnar, 2008; Murdock et al., 1997; Prange and Schulz, 2004; Schneider and Schmittner, 2006; Steph et al., 2010; Zhang et al., 2012; this study)~~. We find that maximum Atlantic Overturning Circulation is ~17.5 Sv, compared to ~18.5 Sv in the modern equivalent (e.g. Ivanovic et al., 2013c), but that in places, North Atlantic Meridional Overturning Circulation is much reduced (i.e. up to 4.8 Sv weaker) than in the modern. Also, the AMOC is completely changed south of the CAS, with strong Southern Ocean sources, due to the opened exchange with the Pacific. We will therefore focus the analysis of the Overturning Circulation and Deep Water Formation on that part of the Atlantic basin which remains enclosed (as captured by Fig. 5~~5~~a). The global annual mean sea surface temperature in *Messinian control* is around 19.8 °C; approximately 2 °C warmer than for the modern (Fig. 4b).

In terms of Mediterranean-Atlantic water exchange, the *Messinian control simulation* preserves the model's modern two-layer flow structure of surface eastward flow of water into the Mediterranean and deeper westward flow into the Atlantic. Around 1.2 Sv of water is exchanged and the flow is enhanced compared to the equivalent modern simulation (Ivanovic et al., 2013c) because the westernmost Mediterranean is on average around 2 psu saltier than for the present day (with a volume integral of around 44 psu), while the easternmost North Atlantic is 1-2 psu fresher (with a volume integral of around 35 psu). Consequently, MOW exports 1.2 psu Sv to the Atlantic, producing a clearly distinguishable, relatively warm, high-salinity plume that spreads westwards in the intermediate-deep North Atlantic (Fig. 6c and d). This comparatively high-salinity plume is similar (although ~0.2 Sv stronger) to that which is observed (e.g. Boyer et al., 2009) and modelled (e.g. Ivanovic et al., 2013c; as shown by Fig. 6a and b) in the modern ocean.

2.3.2 No Mediterranean Outflow Water

Whether or not the Mediterranean ever fully or partially desiccated during the MSC, it seems likely that, at least at times, there was no outflow from the Mediterranean to the Atlantic (e.g.

van Assen et al., 2006; Benammi et al., 1996; Betzler et al., 2006; Hüsing et al., 2010; Ivanovic et al., 2013a; Krijgsman et al., 1999b). Although blocking MOW in a modern HadCM3 simulation had little impact on North Atlantic ocean circulation and climate (Ivanovic et al., ~~in press~~2013c), consistent with other similar GCM simulations (Chan and Motoi, 2003; Kahana, 2005; Rahmstorf, 1998), there is considerable model and proxy evidence to suggest that it has the potential to play a more important role during periods of weaker AMOC (e.g. Bigg and Wadley, 2001; Penaud et al., 2011; Rogerson et al., 2010; Voelker et al., 2006). HadCM3 reproduces the modern AMOC reasonably well; for example, resulting in an overturning strength of 18 ±2 Sv at 26.5° N (Ivanovic et al., ~~in press~~2013c) compared to 18.7 ±5.6 Sv in recent observations (Cunningham et al., 2007). The Messinian HadCM3 AMOC is 4-5 Sv weaker than the modern AMOC, so to investigate whether MOW has a greater effect during weaker AMOC modes than the present day, we ran a 500-year simulation with no Mediterranean-Atlantic water exchange taking place, but with an otherwise identical set-up to the *Messinian control*. We will refer to this simulation as *no-exchange*.

2.3.3 Extreme salinity events

Modern North Atlantic circulation and climate appear to be much more sensitive to extreme changes in MOW salinity than they are to volumetric (and flow-rate) changes in Mediterranean-Atlantic exchange, including total blocking of MOW (Ivanovic et al., ~~in press~~2013c). However, modelled North Atlantic circulation and climate are different in the Messinian compared to the present day (Sects. *2.3.1* and *2.3.2*) and the Mediterranean salinity events thought to have occurred during the MSC are far more extreme than the scenarios examined by Rahmstorf (1998), Bigg and Wadley (2001), Rogerson et al. (2010) or Ivanovic et al. (~~in press~~2013c). The Mediterranean Messinian succession comprises substantial thicknesses of (a) halite and (b) gypsum evaporites, as well as an interval containing (c) near-fresh (or *brackish*) fauna (Fig. 1). Therefore, to assess the potential global-scale influence of the MSC, we ran three sets of extreme salinity simulations, approximately corresponding to the salinity conditions required for (a), (b) and (c) to occur. Note that hereafter, the near-fresh simulations are referred to as *fresh* for simplicity. To ~~force~~ reproduce the changes in Mediterranean salinity, the same method as Ivanovic et al. (~~in press~~2013c) was adopted, ~~holding~~ forcing the entire Mediterranean basin (but nowhere else) ~~at~~ to have constant salinity

~~throughout the run:~~of (a) 380 psu, (b) 130 psu (Flecker et al., 2002) and (c) 5 psu at every timestep for the duration of the run.

The Mediterranean salinity fluctuations that took place during the MSC are widely thought to have been caused by tectonically and climatically driven changes in the volume of Mediterranean-Atlantic exchange water (e.g. Hsu et al., 1977; Krijgsman et al., 1999a). In line with geological evidence and box-modelling (e.g. Flecker and Ellam, 2006; Fortuin and Krijgsman, 2003; Krijgsman and Meijer, 2008; Lugli et al., 2010; Meijer, 2012; Topper et al., 2011), we suggest that a more restricted exchange would generally have resulted in a higher Mediterranean salinity (e.g. gypsum, then halite stauration). However, the variation in exchange volume during Mediterranean hyposalinity is not well understood and the exact exchange rate during any part of the MSC is not yet known. ~~S~~Based on this, simulations were run without changing the coefficient of Mediterranean-Atlantic exchange (μ; the parameterisation of the volume of mixing between the two basins). These will be referred to as (a) *halite-normal*, (b) *gypsum-normal* and (c) *fresh-normal*. In addition, to reflect the likely direction of change (decrease or increase) of~~in~~ MOW volume and flow-rates that would have occurred during the MSC events (discussed above), we also ran a subset of (a), (b) and (c) with appropriate, but idealised changes in the coefficient of exchange (μ); (a) quartering the coefficient for the most saline simulation (*halite-quarter*), (b) halving the coefficient for the less extreme hypersaline simulation (*gypsum-half*) and (c) both halving (*fresh-half*) and doubling (*fresh-double*) the coefficient for the hyposaline scenario because it is difficult to be confident in the direction of change to the exchange volune.~~, as it is not clear how the volume of exchange may have changed during the MSC events~~. The~~All~~ nine simulations are summarised in Table 1.

We acknowledge that of these three scenarios, MOW is least likely to have occurred during halite saturation. Other evidence (incl. Abouchami et al., 1999; Gladstone et al., 2007; Ivanovic et al., 2013a; Meijer and Krijgsman, 2005; Meijer, 2006, 2012; Muiños et al., 2008) indicates that at least episodic bursts of MOW may well have occurred during gypsum saturation~~–~~ and brackish water conditions. Nonetheless, we have tested all three scenarios on the basis that none can yet be disproved; the volume of evaporites found in the Mediterranean Messinian succession cannot be explained without Atlantic inflow and Meijer (2012) shows that a gateway has to be extremely shallow before outflow is blocked.

It should also be noted that holding Mediterranean salinity constant throughout the simulations introduces an unphysical salt source/sink mechanism to the global ocean. Over 500 years, the volume integral for the global ocean salinity changes by around 0.2 psu in *halite-quarter*, 0.1 psu in *gypsum-half* and 0.05 psu in *fresh-normal*. Thus, the changes are small (0.1-0.5 %) and the resulting Mediterranean salt source/sink does not present a problem for understanding the physical mechanisms at work in these idealised simulations. Importantly, the forced constant salinities do mean that changes in global ocean circulation or climate cannot feedback to Mediterranean salinity; investigating this will provide the basis for future work.

Importantly, Atlantic salinity remains below 42 psu in all simulations, even for the grid boxes immediately adjacent to the Spain-Morocco land-bridge during Mediterranean halite and gypsum saturation. This is due to implicit mixing of Mediterranean and Atlantic water in the *pipe* connecting the basins (equation 1) and because the exchange is small compared to the volume of water in each model grid box. Hence, outside of the Mediterranean, ocean salinity stays within the valid range of the models' equation of state (Sect. *2.1*); Mediterranean circulation is not investigated in this study.

3 Results

All climate anomalies presented and discussed here are robust against a student *t*-test with 95 % confidence based on modelled interannual variability, which was calculated for the final 100 years of the simulations.

Formatted: Font: Italic

3.1 No Mediterranean Outflow

In the modern HadCM3 ocean, around 1 Sv of MOW flows westwards through the Gibraltar Straits, whereupon it descends the continental shelf and spreads in a relatively warm plume, centred around 1200-1500 m deep, that is up to 1.8 psu more saline than ambient NACW (Ivanovic et al., ~~in press~~2013c). Whilst not perfect, this is quite a good reproduction of the observed >0.74 ±0.05 Sv of MOW that flows through the Gibraltar Straits into the Atlantic (García-Lafuente et al., 2011) and spreads westwards in a relatively saline (up to +1.8 psu) plume, centred at around 1000-1200 m deep (e.g. Boyer et al., 2009).

Comparing simulations with and without the presence of Mediterranean-Atlantic exchange allows us to examine the MOW contribution to the Atlantic, both in the context of the present day (Ivanovic et al., 2013c) and the Messinian (this study); for example, by using salinity and temperature anomaly plots in *control – noexchange* experiments. This is confirmed by previous simulations with conservative dye tracers (e.g. the work for Ivanovic et al., 2013c), which show that such anomaly plots accurately reflect the spread of MOW in the Atlantic. This also lends credence to the identification of the modern MOW plume in observational datasets (e.g. Boyer et al., 2009) as a tongue of relatively warm, salty water protruding into the Atlantic.

In the Messinian HadCM3 ocean (Fig. 6c and d; this study),~~As it spreads westwards,~~ the 0.2 psu ~~(20 %)~~ saltier ~~and stronger~~ MOW makes a greater contribution to the North Atlantic above 1200 m than it does in the modern (Fig. 6a and b; reproduced from Ivanovic et al., 2013c)~~(Ivanovic et al., in press)~~. Consequently, ~~unlike in the modelled present day ocean, this stronger, more buoyant component of~~ the MOW plume becomes entrained in the shallower, northward flowing currents of the AMOC and reaches further north. This means it ~~,~~ ~~making~~ makes a greater direct contribution to the Greenland-Iceland-Norwegian, GIN, and Barents Seas (locations indicated by Fig. 2)~~. As a result, MOW reaches further north,~~ and also ~~providing~~ provides relatively warm, salty water to sites of central North Atlantic upwelling. Thus the difference in MOW buoyancy between the Messinian and present day is important in regulating its wider impact. ~~However, w~~We also find that the absence of MOW in *no-exchange* reduces Messinian AMOC by ~ 2 Sv~~up to 3 Sv~~ (~~13-30 %;~~ Fig. 5~~5~~b), compared to ~~only 1~~0.7 Sv~~ (up to 16 %)~~ in the modern ocean (Ivanovic et al., ~~in press~~2013c). In agreement with Bigg and Wadley (2001), Voelker et al. (2006), Rogerson et al. (2006, 2010, 2012), Penaud et al. (2011) and others, this suggests that MOW does indeed have a greater effect on North Atlantic Ocean circulation during weaker modes of AMOC than it does under the stronger, present-day regime.

~~In addition, we note that deeper components of the plume remain in the simulation, and because overall these are also stronger and more saline than for the present, Messinian MOW makes a greater contribution to the southward flowing, exporting currents than in the modern ocean. Without MOW feeding salty water to the exporting arm of the AMOC and with the weakened NADW formation, there is a reduced supply of relatively deep, saline waters to the Southern Ocean. Consequently, Antarctic Bottom Water (AABW) formation is also reduced by 14-57 % (up to 5 Sv). This in turn affects overturning circulation in the Pacific basin, decreasing the spread of AABW at intermediate depths by 10-20 % (up to 2 Sv; Fig. 5b).~~

Without MOW in the North Atlantic in *no-exchange*, less relatively warm, salty water reaches sites of upwelling and therefore, cooler, fresher water is brought to the surface ~~in *no-exchange*~~ than in *Messinian control* (Fig. ~~6~~7). A site centred at around 50° N, 40° W is particularly affected by this, where the upwelling of relatively colder water in *no-exchange* cools the overlying atmosphere by up to ~~1~~ 0.9 °C (annual mean Surface Air Temperature, SAT) relative to *Messinian control*~~, producing a North Atlantic 'coldspot'.~~ . ~~The effect is enhanced during the Boreal winter-spring, when the region is cooled by up to 1.5 °C.~~ Furthermore, with a weakened AMOC and a cooler, fresher intermediate North Atlantic (e.g. Fig. 7d), ~~there is a decrease in the northward flow of~~less relatively warm, salty, shallow-intermediate, low latitude water reaches the higher northern latitudes and there is reduced exchange between the Atlantic and the GIN Seas. In the subsurface, this results in cooling (and freshening) of the GIN and Barents Seas (Fig. ~~6~~7), with the temperature signal being transferred upwards to cause an overal cooling of up to 1 °C (annual mean SAT) in the~~the~~ overlying atmosphere~~. Consequently, sea-ice formation is boosted in these regions, which increases the local surface albedo, positively feeding back to the initial temperature change.~~

~~This feedback results in a regional cooling of up to 1.2 °C (annual mean SAT) and an increase in sea-ice coverage of up to 10 % (up to 2.5 °C and 25 % in the Boreal winter-spring, respectively)~~. ~~The increase in sea-ice coverage and the reduction in the supply of relatively warm, salty lower latitude water decreases vertical mixing in the GIN and Barents Sea, reducing NADW formation in the region and shoaling the mixed layer by up to 130 m during the Boreal winter (up to 55 m for the annual mean).~~ The reduced exchange between the Atlantic and GIN Seas means less relatively cold, high latitude water escapes southwards from the GIN Seas and consequently, ~~also results in (~~the shallow~~)~~ ocean off the Greenland coast and in the Labrador Sea is ~1 °C warmer than in *Messinian control* ~~warming of up to 2 °C off the Greenland coast and in the Labrador Sea~~ (warming seen in Fig. ~~6a~~ 7a and b~~, location indicated by Fig. 2~~)~~,~~. ~~and~~ Warming of ~1 °C also occurs along the Atlantic's eastern boundary (Fig. ~~6c~~7c) where cooler high-latitude water (e.g. from the GIN Seas) has been replaced by relatively warm, Atlantic water, with respect to *Messinian control*. However, little of this warming signal is transferred to the surface ocean (Fig. ~~6a~~7a) and there is no statistically significant imprint on surface air temperatures.

3.2 Extreme salinity events

In order to assess the robustness of the model results, seven Mediterranean salinity simulations were run in total (Table 1); two halite saturation scenarios (*halite-normal* and *halite-quarter*), two gypsum saturation scenarios (*gypsum-normal* and *gypsum-half*) and three brackish lagoon scenarios (*fresh-half*, *fresh-normal* and *fresh-double*). A detailed analysis was carried out on all seven of these simulations and the full data can be accessed at http://www.bridge.bris.ac.uk/resources/simulations. However, for each high/low Mediterranean salinity scenario (380 psu, 130 psu, 5 psu), the results were remarkably similar. Generally, the climate anomalies had the same direction of change and were brought about through the same mechanisms, although the magnitude of change was different depending on the exchange strength (varied μ, see Table 1); reducing the exchange damped the anomalies, enhancing the exchange exaggerated the anomalies. Therefore for clarity, the following discussion is focused on the three most pertinent simulations (one per set of scenarios). For the hypersaline-Mediterranean scenarios we chose those simulations with a direction of change in the coefficient of exchange (μ) that best represents the physical constriction of the gateways that is most likely to have occurred (see the discussion in Sect. 2.3.3); this is *halite-quarter* and *gypsum-half*. These reduced-exchange simulations also produce far less extreme (though still very large) salinity fluxes through the gateways than their unrestricted (i.e. unchanged μ) counterparts, *halite-normal* and *gypsum-normal* (Table 1). For the hyposaline-Mediterranean scenarios the most appropriate simulation to discuss~~is~~ is *fresh-normal*. This is because we do not know whether Mediterranean-Atlantic exchange increased or decreased during these events. All anomalies are given with respect to *Messinian control*.

Formatted: Font: Not Italic

3.2.1 Mediterranean Hypersalinity

The model responds to extreme increases in Mediterranean (Outflow Water) salinity by enhancing the two-layered Mediterranean-Atlantic exchange (1.2 Sv in *Messinian control*) by approximately 10 Sv in *halite-quarter* ~~-~~and 5.3 Sv in *gypsum-half*. The imposed, uniform haline forcing (Table 1) of the experiment design causes a reduction in downward mixing of relatively warm Mediterranean surface waters and ~~This results in~~induces cooling of the Mediterranean basin, ~~(~~on average by around 2.0 °C in *halite-quarter* and 1.8 °C in *gypsum-half*. In addition, the increased exchange with the Atlantic ~~) and also~~ elevates Mediterranean salt export (1.2 psu Sv in *Messinian control*) by 19.4 psu Sv and 9.8 psu Sv, respectively (Table 1). Mainly a~~A~~s a result of its salting, MOW becomes much stronger and denser, deepening in the North Atlantic and spreading predominantly southwards from the Mediterranean-Atlantic corridors ~35° N (e.g. Fig. ~~7a~~ 8a and b)~~, where it becomes entrained~~

~~in the Antarctic Circumpolar Current and proceeds to mix with the global ocean~~. Although the MOW plume is cooler than in *Messinian control*, it is also saltier, so that at neutral buoyancy it resides in less saline, cooler Atlantic water. Thus overall, the salinity and temperature of the intermediate-deep Atlantic and Southern Oceans is raised.

This has effectively shifted a component of NADW formation to the Mediterranean basin. In *halite-quarter* and *gypsum-half*, NADW formation is weakened by up to 5.6 Sv ~~(~38 %)~~ and ~~8~~ 7.7 Sv~~ (~50 %)~~, respectively, while the AMOC south of 35° N is strengthened by around ~~up to 6~~7 Sv ~~(~55 %)~~ and ~~3~~1.5 Sv~~ (~18 %)~~; Fig. ~~5c~~ 5c and d. ~~This increase in the salinity and strength of southward flowing intermediate-deep currents feeds AABW formation, strengthening it by up to 22 Sv.~~

~~In the Northern Hemisphere, t~~These changes in mid-high latitude ocean overturning circulation reduce the poleward ~~shallow~~ transport of shallow, relatively warm and~~,~~ salty low-latitude waters ~~in the Atlantic~~ north of the Mediterranean-Altantic corridors ~35° N and as a consequence, parts of the high latitude North Atlantic-Labrador-GIN Seas region cool by a few degrees (See Fig. 9b and c)~~. In addition, the strong eastward draw of shallow-intermediate waters across the North Atlantic and into the Mediterranean (from enhanced Mediterranean-Atlantic exchange) entrains and accelerates subpolar and subtropical gyre currents (present day configurations schematically illustrated by Fig. 2). As a result, the strengthened subpolar gyre deepens by >330 m, elongates along a northwest-southeast axis and shrinks across its northeast-southwest axis, so that it reaches further into the Labrador Sea, but withdraws from the Greenland-Iceland-Scotland Ridge. The decrease in shallow-intermediate AMOC flow (and NADW formation) north of 35° N and the south-eastward migration of the (stronger) subpolar gyre weakens Atlantic-GIN Seas water exchange, but enhances flow between the Labrador Sea and Atlantic. Curtailed Atlantic-GIN Seas connectivity substantially cools the GIN and Barents Seas throughout the surface-intermediate water column. This effect is enhanced by the reduced poleward heat transfer north of 35° N. Furthermore, enhanced exchange between the Labrador Sea and Atlantic Ocean replaces the flow of relatively warm, mid-latitude water into the Labrador Sea with the now cooler Atlantic flow. It also increases the transport of relatively cold, high latitude Labrador Sea water south towards the mid latitudes, reducing North Atlantic water temperature even more~~.

~~The cooling of the mid-high latitude North Atlantic, Labrador, GIN and Barents Seas is transferred to the overlying atmosphere. As a result of the decrease in both sea surface and~~

~~SATs, sea-ice formation in the high latitude northern Hemisphere increases, positively feeding back into the initial cooling trend, which spreads; reaching over the Eurasian and North American continents and propagating into the high-latitude Pacific.~~ The North Atlantic subtropical gyre transports this ~~oceanic~~ cooling signature southwest across the North Atlantic, towards the open CAS. ~~Consequently, Northern Hemisphere mid-high latitude SATs decrease by up to 4 °C for both *halite-quarter* (Fig. 8b) and *gypsum-half* (Fig. 8c), corresponding to an increase in sea-ice cover of 30 %. These annual mean SAT (and sea-ice formation) anomalies are enhanced during the Boreal winter-spring, reaching up to -9 °C and +60 %, respectively.~~

Similar to *no-exchange*, in *gypsum-half*,~~the~~ reduced subsurface outflow from the GIN Seas to the North Atlantic actually results in localised shallow warming of a small area in the northernmost North Atlantic, south of Greenland. This transfers to the overlying atmosphere and increases annual mean SATs by up to 1.4~~5~~ °C (Fig. ~~8c~~9c). By the same process, eastern boundary intermediate water is also warmed by up to 1.7~~2.5~~ °C (annual mean), but this is too deep to be transferred to surface water or air temperatures. H~~owever, h~~igh-latitude cooling in the other hypersaline-Mediterranean simulations (including *halite-quarter*), is so strong that it overrides this surface air-temperature warming and only cooling is observed in the region (e.g. Fig. ~~8b~~9b).

~~Upon reaching very dense, cold AABW in the South Atlantic and Southern Ocean, some of the relatively warm, saline, Mediterranean-origin waters shoal and are brought to the surface in both *halite-quarter* and *gypsum-half*. Where this occurs, the density gradient in the upper 600 m is reduced and the annual mean mixed layer deepens by up to 65 m (125 m in the Austral winter). Relative warming of the surface ocean heats the overlying atmosphere, producing pockets of warmer SATs over the Southern Ocean. As a result, up to 20 % less sea-ice is formed (annual mean) in the Weddell, Davis and Amundsen Seas around Antarctica and consequently, the sea-ice albedo feedback enhances warming in these regions (particularly in *halite-quarter*). This causes the overlying surface air to warm by up to 2.5 °C for *halite-quarter* (Fig. 8b) and *gypsum-half* (Fig. 8c). The elevated salinity of the Antarctic Circumpolar Current in *halite-quarter* and *gypsum-half* supplies the Pacific with denser water, switching on weak deep water formation in the Pacific sector of the Southern Ocean, thus strengthening the upwelling of cold, deep water in the South Pacific between 40° S to 60° S and 120° E to 150° W. This causes localised sea surface temperatures in these areas to drop by up to 3 °C (annual mean anomaly), also cooling the overlying atmosphere by up to 3 °C~~

~~(annual mean; e.g. Fig. 8b and c).~~

3.2.2 Mediterranean Hyposalinity

Freshening the Mediterranean in *fresh-normal* both reverses and steepens the density gradient between the Mediterranean and the Atlantic, resulting in an opposite two-layer exchange-structure (surface westward flow and deeper eastward flow) that has been enhanced by 6.3 Sv. Consequently, the Mediterranean cools, on average, by around 4.0 °C. However, it also becomes a salinity sink (or freshwater source) to the Atlantic, now importing around 7.0 psu Sv, compared to the export of 1.2 psu Sv in *Messinian control*. This more than counteracts the reduction in MOW buoyancy (increase in MOW density) arising from Mediterranean cooling and freshens the entire North Atlantic water column (Fig. ~~7c~~8c). In particular, this affects the shallow (0-400 m) levels that now receive this brackish-water injection from the Mediterranean and the intermediate-deep levels (800-2000 m) that are now without the relatively saline MOW plume that is present in *Messinian control*.

Unlike the modern *fresh-Med* simulations run by Ivanovic et al. (~~in press~~2013c), the effect on Atlantic Ocean circulation is rather straight forward, profound and widespread. This is mainly due to the relatively weaker AMOC (by 2.7-4.8~~4-5~~ Sv) compared to the present day and the more important role MOW played in governing Messinian overturning circulation (Sect. *3.1*) with respect to the modern (Ivanovic et al., ~~in press~~2013c). Interestingly, although our Mediterranean salinity perturbation is 15 psu larger than the Mediterranean freshening simulations run by Ivanovic et al. (~~in press~~2013c), this plays only a very minor role in generating the difference between the modern and Messinian climate anomalies. Modern simulations with a 5 psu Mediterranean (unpublished data, available at http://www.bridge.bris.ac.uk/resources/simulations) show anomaly patterns with the same locality and direction of change as with a 19 psu Mediterranean (warming in the GIN Seas, cooling in the North Atlantic, but no further-spread climate signal; Ivanovic et al., ~~in press~~2013c), but are of greater magnitude. In the Messinian simulations, freshening of the shallow-intermediate North Atlantic causes a total collapse of NADW formation and the AMOC (Fig. ~~5e~~5e). ~~Subsequent freshening of the Southern Ocean through reduced southward transport of relatively saline intermediate-deep water also weakens AABW formation in the Southern Ocean by 15 Sv and reduces Pacific Meridional Overturning Circulation by 8 Sv.~~

The collapse of the AMOC and consequent reduction in northward heat transport from the equator in the shallow-intermediate North Atlantic more than counteracts any warming from the increased direct supply of more southerly-sourced, shallow water to the GIN Seas (e.g. Sect. 3.3.1 and Fig. 6b in Ivanovic et al., ~~in press~~2013c), especially as MOW itself is now cooler. The resulting annual mean high latitude cooling of up to 8 °C in the shallow-intermediate subsurface (e.g. Fig. ~~9a~~ 10a and b) is transferred to the overlying atmosphere~~ and local sea-ice formation increases, amplifying the initial cooling trend. This reduces annual mean SATs by up to 9 °C (Fig. 8d) and increases sea-ice cover by up to 40 %. This polar amplification allows the cold-anomaly to spread southwards~~, causing widespread cooling of 1-3 °C (and up to 8 °C in places) in the Northern Hemisphere, even reaching across the equator in a few locations; over the African continent, Brazil, Australia and the mid-Pacific (Fig. ~~8~~9d). In addition, the North Atlantic subtropical gyre transports relatively cold, shallow water (including a direct contribution from MOW) southwest across the North Atlantic, through the open CAS and into the Pacific (Fig. ~~9a~~10a), creating a relatively cool, low-latitude current that can be seen in the SAT anomalies (Fig. ~~8d~~9d).

Conversely, parts of the Southern Hemisphere are warmer in *fresh-normal*, compared to *Messinian control*. This *bipolar* phenomenon has also been instigated by the collapse of the AMOC, whereby relatively cold NADW is no longer transported south, at depth, to the Southern Ocean. As a result, the intermediate-deep South Atlantic, Southern and Indian Oceans are up to 2 °C warmer than in *Messinian control* (Fig. ~~9c~~10c). This warming is transferred to the surface ocean at sites of upwelling (e.g. Fig. ~~9a~~ 10a and b), resulting in SAT anomalies of ~~around 1~~0.7-1.0 °C in these regions (Fig. ~~8d~~9d). In addition, weak, very deep AABW formation in the Pacific sector of the Southern Ocean (Amundsen Sea) is switched on in the hyposaline-Mediterranean simulations and there is an overall reduction in South Pacific upwelling. Thus, where upwelling in the *Messinian control* brings relatively cold, Pacific deep (and bottom) water through the water column towards the surface, with a hyposaline-Mediterranean the intermediate-shallow South Pacific becomes ~~up to~~ 0.5-2.~~5~~7 °C warmer (Fig. ~~9b~~10b), heating the air above by ~~up to 1.5~~0.5-1.9 °C (Fig. ~~8d~~9d).

In the Pacific, there is also reduced transport of relatively saline, low-latitude surface waters south. This raises equatorial surface water salinity and contributes towards water column instability, boosting the strength of a latitudinally-narrow overturning cell in the region. This mixes relatively warm, shallow water down through the water column, warming the Pacific equatorial subsurface by up to 6.5 °C (e.g. Fig. ~~9b~~10b). Thus, heat from the equator is transferred downwards, rather than polewards. Subsurface, eastward flow through the open

Formatted: Not Highlight

Formatted: Not Highlight

CAS carries some of this warmer water into the Caribbean Sea and Gulf of Mexico (locations indicated by Fig. 2), but the positive temperature anomaly is confined here and does not reach the open Atlantic (Fig. ~~9b~~10b). This process also occurs in the Indian Ocean, but to a lesser extent. ~~Notably, Southern Hemisphere air temperature anomalies are greatest off the Antarctic coast (Fig. 8d), where warming decreases sea-ice formation (therefore reducing surface albedo) and positively feeds back to the initial climate perturbation.~~

Neither of the hypersaline-Mediterranean simulations (*halite-quarter* and *gypsum-half*) show a discernible reorganis~~z~~ation of atmospheric circulation with respect to *Messinian control*, nor do they have a significant effect on precipitation. Conversely, the bipolar Northern Hemisphere cooling and Southern Hemisphere warming of the hyposaline simulations does induce a 2° (approx.) southward shift of~~–~~ precipitation falling along the northern edge of the inter-tropical convergence zone. This signal is strongest over the Pacific, where the northern tropics dry and the southern tropics moisten by up to ~~8~~ 6 mm day^{-1}. Importantly, the affected regions have also been influenced by the reduction in poleward thermal/haline transports, causing a build-up of heat and salt near the equator. The southward shift in precipitation-evaporation over the tropics enhances the local salinity anomalies that result in the~~a~~ latitudinally narrow convection cell discussed above.

4 Discussion and conclusions

In our HadCM3 simulations, blocking Mediterranean-Atlantic exchange during the Messinian Salinity Crisis reduces AMOC ~~and AABW formation~~ strength by up to ~~3~~ 2.3 Sv~~ and 5 Sv, respectively~~. This is different~~contrary~~ to HadCM3 simulations of the modern ocean without MOW, which instead show a smaller ~~strengthening~~ weakening (~~1~~ 0.7 Sv) ~~only~~ in deep AMOC components south of the Gibraltar Straits that is concurrent with a small (1-2 Sv) ~~and no change to AABW formation, although there is a small~~ strengthening of NADW formation~~(1-2 Sv) concurrent weakening of NADW~~ (Ivanovic et al., ~~in press~~2013c). The modern climate is seemingly insensitive to the presence of MOW in the North Atlantic (e.g. Artale et al., 2002; Chan and Motoi, 2003; Ivanovic et al., ~~in press~~2013c; Kahana, 2005; Rahmstorf, 1998; Wu et al., 2007), but the Messinian AMOC's response to blocking MOW produces very localised SAT cooling of up to ~~1~~ 0.9 °C over the central North Atlantic Ocean and GIN Seas and up to 1~~.2~~ °C over the Barents Sea~~ (2.5 °C in the Boreal winter-spring)~~. These differences between the Messinian and the modern arise from (a) Messinian MOW making a greater contribution to the upper 1200 m in the North Atlantic due to raised Atlantic salinity compared to the

Formatted: Not Highlight

Formatted: Not Highlight

Formatted: Not Highlight

Formatted: Not Highlight

modern and (b) the weaker Messinian AMOC (and its influence on climate) being more susceptible to Atlantic salinity and temperature perturbations; in this instance, the absence of Mediterranean-origin water.

The Mediterranean-salinity perturbations have a much greater and widespread impact on climate, with consistency in the results across all seven simulations (Table 1). *Halite-quarter* and *gypsum-half*, which are probably the most realistic of the hypersalinity simulations (see the discussions in Sects. 2.3.3 and 3.2), both have a very similar affect on ocean circulation and climate compared to *Messinian control*. Broadly, elevating Mediterranean salinity enhances Mediterranean-Atlantic exchange and salt export, shifting a component of deep water formation out of the North Atlantic and into the Mediterranean. This weakens NADW formation ~~(~~by 5~~6~~-8 Sv~~), but strengthens both the AMOC south of 35° N (by 3-7 Sv) and AABW formation (by up to 22 Sv)~~. The resulting impact on water exchange between the North Atlantic and high latitude seas, combined with the more global effect on ocean heat transport cools Northern mid-high latitude SATs by ~~up to 4 °C~~a few degrees~~ (9 °C in the Boreal winter-spring)~~.

Formatted: Not Highlight

In addition, the reduced exchange between the North Atlantic and GIN Seas in *gypsum-half* causes some localised warming of up to 1.7~~2.5~~ °C in the shallow-intermediate northernmost North Atlantic Ocean (warming the overlying air) and along the North Atlantic eastern boundary. This also takes place with a blocked Mediterranean-Atlantic exchange, but in the other hypersaline-Mediterranean simulations, including *halite-quarter*, surface cooling is too strong and overrides any relative warming that may take place. It is important to consider that these results may be influenced by the overly diffuse MOW plume simulated by HadCM3. For example, a more coherent MOW core would probably not interact with intermediate and deep Atlantic Ocean circulation as significantly as in these simulations, but would instead sink and pool at the bottom of the North Atlantic. On the other hand, this effective enhancement of North Atlantic entrainment in MOW could be an important counteraction to the underestimation of shallow-intermediate mixing between MOW and NACW in what is now the Gibraltar Straits-Gulf of Cadiz region.

Formatted: Not Highlight

Brackish-MOW in the hyposaline-Mediterranean simulations produces a bipolar climate signal, with widespread cooling of 1-3 °C (and up to ~~9~~ 8 °C) in Northern Hemisphere SATs and patchy-warming of 0.5-2.7~~(up to 2.5~~ °C~~)~~ at sites of intermediate-deep water upwelling in the Southern Hemisphere. These temperature anomalies are predominantly caused by AMOC

Formatted: Not Highlight

collapse (in response to Atlantic freshening by Mediterranean-origin water), which reduces northward heat-transfer in the shallow ocean and stops relatively cold NADW from being transferred South in the intermediate-deep layers. Notably, these effects are much greater and, in the GIN Seas, are even opposite in direction to the anomalies simulated with a 5 psu Mediterranean and a modern (pre-industrial) model configuration. The hyposaline-Mediterranean simulations are the only simulations to exhibit changes in precipitation patterns beyond interannual variability; a southward shift, by a few degrees, of the inter-tropical convergence zone. This shift and the bipolar climate anomalies, both predominantly caused by AMOC collapse, are consistent with (if larger than) results from high northern latitude freshwater-hosing experiments (e.g. Clement and Peterson, 2008; Kageyama et al., ~~2012~~2013; Stouffer et al., 2006; Zhang and Delworth, 2005).

The conditions of Mediterranean-Atlantic exchange modelled here in the hyper- and hypo-saline experiments are not meant to represent realistic MSC scenarios. Rather, they have been designed to push the limits of the climate response to very extreme instances of changes in MOW conditions. The enhanced exchange strength simulated in this study (~11.2 Sv for *halite-quarter*, 6.5 Sv for *gypsum-half* and 7.5 Sv for *fresh-normal*) are unlikely conditions for sustained halite saturation, gypsum saturation or brackish Mediterranean water conditions in the MSC (e.g. Garcia-Castellanos and Villaseñor, 2011; Meijer, 2012; Topper et al., 2011). Instead, events of extremely elevated or negative Mediterranean salt-export are most likely to have occurred intermittently (as postulated by Thierstein and Berger, 1978), for example at the end of each episode of Mediterranean high/low-salinity. Such hyper-/hypo-saline transition phases between normal marine and extreme Mediterranean conditions are in contrast to the forced, constant extreme salinity MOW events modelled in this sensitivity study. However, if considering Messinian MOW hyper- and hypo-salinity as a series of short events, time series information from some of our coupled AOGCM simulations (available at http://www.bridge.bris.ac.uk/resources/simulations) suggests that initially, there is a decadal scale overshoot in ocean circulation. It therefore seems likely that the shorter-term (transient) ocean circulation impact of MSC events could actually be far more extreme than the results discussed here. We have not aimed to explore the early time-series response of the global ocean to the MSC, these simulations are 'equilibrium' experiments, but future work could focus on transient scenarios to examine a more realistic timeline of events. Currently, this is difficult as we do not have sufficient evidence to constrain the evolution of Mediterranean-Atlantic connectivity during the MSC. However, new data (Ivanovic et al., 2013a) provides some hope that this could soon be rectified.

Data coverage for the late Miocene is sparse and patchy (Bradshaw et al., 2012). We suggest that the global-scale MSC climate signal could be absent (e.g. discussions within Murphy et al., 2009; Schneck et al., 2010) due to palaeo-climate reconstructions inadvertently targeting either the wrong geographic locations or the wrong climate variables. In addition, the reconstructions may have insufficient temporal resolution to distinguish the events. With these, fully-coupled GCM simulations, we have begun to address these possibilities, providing key information on which geographical regions and climate variables are most susceptible to possible MSC-induced perturbations. Appropriate proxy archives and sample locations can be identified and targeted for geologic evidence of global-scale climate change brought about by Messinian Mediterranean hyper/hypo-salinity and blocked-MOW scenarios. Such data would not only provide a more robust test for global general circulation models and our process-based understanding of climate interactions (including the influence of MOW on North Atlantic circulation and climate), but would also lead to a better knowledge of MSC Mediterranean-Atlantic connectivity in the absence of more conclusive data (Abouchami et al., 1999; Ivanovic et al., 2013a; Muiños et al., 2008). North Atlantic sea surface and surface air temperatures consistently show the most variability in all eight of our MSC-scenario simulations; whether there is no Mediterranean-Atlantic exchange, or hyper/hyposaline MOW (Fig. 9).

~~The climate variable that consistently shows the most change between the different MSC simulations is temperature, for which the anomalies are relatively large, usually geographically widespread and always statistically significant. There are some key regions for which SAT and ocean temperatures are affected in all simulations; parts of the GIN and Barents Seas, the northernmost and central North Atlantic and, for some simulations, the east Atlantic (offshore Northwest Africa and Portugal), the South Atlantic (offshore Namibia) and the South Pacific (near New Zealand). Therefore, surface air and ocean temperature reconstructions for these locations (best identified and more accurately constrained by Figures 6, 8 and 9) would make an excellent database for evaluating model performance and examining the evolution of Mediterranean-Atlantic connectivity over the MSC; during which events was there Mediterranean outflow to the Atlantic? Some regions make particularly good test cases because the temperature changes are opposite in direction for different Mediterranean-salinity perturbations; for example, *gypsum-half* has a warmer northernmost~~

~~North Atlantic than *Messinian control*, but *halite-quarter* and *fresh-normal* are cooler; whereas around New Zealand, both *halite-quarter* and *gypsum-half* are cooler than *Messinian control*, but *fresh-normal* is warmer.~~ We therefore propose that by focusing ~~on~~ Messinian temperature reconstructions ~~at these~~on this ~~target~~ ~~locations~~region, future proxy-archive work could more definitively establish whether or not the MSC had the global-scale climate impact that our model results suggest it could have.

Acknowledgements

This work was funded by a University of Bristol Centenary Scholarship and was carried out using the computational facilities of the Advanced Computing Research Centre, University of Bristol, http://www.bris.ac.uk/acrc/. Full access to the data produced by these simulations is provided at http://www.bridge.bris.ac.uk/resources/simulations. We are very grateful to two anonymous reviewers for their valuable comments on the manuscript, and to Yves Godderis for swift editorial handling.

Formatted: Space Before: 0 pt, Line spacing: Double, Widow/Orphan control, Don't adjust space between Latin and Asian text, Don't adjust space between Asian text and numbers

Formatted: Font: (Default) Times New Roman, 12 pt, Font color: Black, German (Germany)

Formatted: Font: (Default) Times New Roman, 12 pt, Font color: Black, German (Germany)

Formatted: Font: (Default) Times New Roman, 12 pt, Font color: Black, German (Germany)

Formatted: Font: (Default) Times New Roman, 12 pt, Font color: Black, German (Germany)

References

Abouchami, W., Galer, S. J. . and Koschinsky, A.: Pb and Nd isotopes in NE Atlantic Fe–Mn crusts: Proxies for trace metal paleosources and paleocean circulation, Geochim. Cosmochim. Acta, 63(10), 1489–1505, doi:10.1016/S0016-7037(99)00068-X, 1999.

Artale, V., Calmanti, S. and Sutera, A.: Thermohaline circulation sensitivity to intermediate-level anomalies, Tellus A, 54(2), 159–174, doi:10.1034/j.1600-0870.2002.01284.x, 2002.

Van Assen, E., Kuiper, K. F., Barhoun, N., Krijgsman, W. and Sierro, F. J.: Messinian astrochronology of the Melilla Basin: Stepwise restriction of the Mediterranean-Atlantic connection through Morocco, Palaeogeogr. Palaeoclimatol. Palaeoecol., 238(1-4), 15–31, doi:16/j.palaeo.2006.03.014, 2006.

Benammi, M., Calvo, M., Prévot, M. and Jaeger, J.-J.: Magnetostratigraphy and paleontology of Aït Kandoula basin (High Atlas, Morocco) and the African-European late Miocene terrestrial fauna exchanges, Earth Planet. Sci. Lett., 145(1–4), 15–29, doi:10.1016/S0012-821X(96)00183-5, 1996.

Benson, R. H., Bied, K. R.-E. and Bonaduce, G.: An important current reversal (influx) in the Rifian Corridor (Morocco) at the Tortonian-Messinian boundary: The end of Tethys Ocean, Paleoceanography, 6(1), P. 165-192, doi:199110.1029/90PA00756, 1991.

Bethoux, J. P. and Gentili, B.: Functioning of the Mediterranean Sea: past and present changes related to freshwater input and climate changes, J. Mar. Syst., 20(1–4), 33–47, doi:10.1016/S0924-7963(98)00069-4, 1999.

Betzler, C., Braga, J. C., Martín, J. M., Sánchez-Almazo, I. M. and Lindhorst, S.: Closure of a seaway: stratigraphic record and facies (Guadix basin, Southern Spain), Int. J. Earth Sci., 95(5), 903–910, doi:10.1007/s00531-006-0073-y, 2006.

Bigg, G. R. and Wadley, M. R.: Millennial-scale variability in the oceans: an ocean modelling view, J. Quat. Sci., 16(4), 309–319, doi:10.1002/jqs.599, 2001.

Blanc, P.-L.: Of sills and straits: a quantitative assessment of the Messinian Salinity Crisis, Deep Sea Res. Part Oceanogr. Res. Pap., 47(8), 1429–1460, doi:10.1016/S0967-0637(99)00113-2, 2000.

Böhme, M., Ilg, A. and Winklhofer, M.: Late Miocene “washhouse” climate in Europe, Earth Planet. Sci. Lett., 275(3–4), 393–401, doi:10.1016/j.epsl.2008.09.011, 2008.

Boyer, T. P., Antonov, J. I., Baranova, O. K., Garcia, H. E., Johnson, D. R., Locarnini, R. A., Mishonov, A. V., O’Brien, T. D., Seidov, D., Smolyar, I. V. and Zweng, M. M.: World Ocean Database 2009, NOAA Atlas NESDIS 66, edited by: Levitus, S., US Gov. Printing Office, Washington D.C., 216 pp., 2009.

Bradshaw, C. D., Lunt, D. J., Flecker, R., Salzmann, U., Pound, M. J., Haywood, A. M. and Eronen, J. T.: The relative roles of CO2 and palaeogeography in determining late Miocene

Formatted: Bibliography, Justified, Widow/Orphan control, Adjust space between Latin and Asian text, Adjust space between Asian text and numbers

climate: results from a terrestrial model–data comparison, Clim Past, 8(4), 1257–1285, doi:10.5194/cp-8-1257-2012, 2012.

Bryan, K. and Cox, M. D.: An Approximate Equation of State for Numerical Models of Ocean Circulation, J. Phys. Oceanogr., 2(4), 510–514, doi:10.1175/1520-0485(1972)002<0510:AAEOSF>2.0.CO;2, 1972.

Canals, M., Puig, P., Madron, X. D. de, Heussner, S., Palanques, A. and Fabres, J.: Flushing submarine canyons, Nature, 444(7117), 354–357, doi:10.1038/nature05271, 2006.

Cattle, H., Crossley, J. and Drewry, D. J.: Modelling Arctic Climate Change [and Discussion], Philos. Trans. Phys. Sci. Eng., 352(1699), 201–213, 1995.

Chan, W.-L. and Motoi, T.: Effects of Stopping the Mediterranean Outflow on the Southern Polar Region, Polar Meteorol Glaciol Nat Inst Polar Res, (17), 25–35, 2003.

Clement, A. C. and Peterson, L. C.: Mechanisms of abrupt climate change of the last glacial period, Rev. Geophys., 46(4), n/a–n/a, doi:10.1029/2006RG000204, 2008.

Cox, P. M., Betts, R. A., Bunton, C. B., Essery, R. L. H., Rowntree, P. R. and Smith, J.: The impact of new land surface physics on the GCM simulation of climate and climate sensitivity, Clim. Dyn., 15(3), 183–203, doi:10.1007/s003820050276, 1999.

Cunningham, S. A., Kanzow, T., Rayner, D., Baringer, M. O., Johns, W. E., Marotzke, J., Longworth, H. R., Grant, E. M., Hirschi, J. J.-M., Beal, L. M., Meinen, C. S. and Bryden, H. L.: Temporal Variability of the Atlantic Meridional Overturning Circulation at 26.5°N, Science, 317(5840), 935–938, doi:10.1126/science.1141304, 2007.

Decima, A. and Wezel, F.: Late Miocene evaporites of the Central Sicilian Basin, DSDP Leg 13 Init Rep, 13, 1234–1240, 1973.

Demicco, R. V., Lowenstein, T. K. and Hardie, L. A.: Atmospheric pCO2 since 60 Ma from records of seawater pH, calcium, and primary carbonate mineralogy, Geology, 31(9), 793–796, doi:10.1130/G19727.1, 2003.

Dowsett, H. J., Barron, J. A., Poore, R. Z., Thompson, R. S., Cronin, T. M., Ishman, S. E. and Willard, D. A.: Middle Pliocene Paleoenvironmental Reconstruction: PRISM2, USGS Open File Rep., 99-535, available at: http://pubs.usgs.gov/of/1999/of99-535/ (last access: 20 May 2013), 1999.

Dowsett, H. J. and Cronin, T. M.: High eustatic sea level during the middle Pliocene:Evidence from the southeastern U.S. Atlantic Coastal Plain, Geology, 18(5), 435–438, doi:10.1130/0091-7613(1990)018<0435:HESLDT>2.3.CO;2, 1990.

Duggen, S., Hoernle, K., van den Bogaard, P., Rüpke, L. and Phipps Morgan, J.: Deep roots of the Messinian salinity crisis, Nature, 422(6932), 602–606, doi:10.1038/nature01553, 2003.

Dutay, J.-C., Sepulchre, P., Arsouze, T. and Jaramillo, C.: Modeling Nd oceanic cycle in present and past climate, with a focus on the closure of the Panama isthmus during the Miocene, oral presentation at the 22nd Goldschmidt Geochemistry Conference, Montreal (Canada), 24–29 June, 2012.

Dvorkin, Y., Lensky, N. G., Lyakhovsky, V. and Gavrieli, I.: Description and benchmarking of the 1D multi-component chemistry-based model for the Dead Sea (1D-DS-POM), Ministry of National Infrastructures, Geological Survey of Israel, Jerusalem, 2007.

Edwards, J. M. and Slingo, A.: Studies with a flexible new radiation code. I: Choosing a configuration for a large-scale model, Q. J. R. Meteorol. Soc., 122(531), 689–719, doi:10.1002/qj.49712253107, 1996.

Flecker, R. and Ellam, R. M.: Identifying Late Miocene episodes of connection and isolation in the Mediterranean-Paratethyan realm using Sr isotopes, Sediment. Geol., 188-189, 189–203, doi:16/j.sedgeo.2006.03.005, 2006.

Flecker, R., de Villiers, S. and Ellam, R. .: Modelling the effect of evaporation on the salinity–87Sr/86Sr relationship in modern and ancient marginal-marine systems: the Mediterranean Messinian Salinity Crisis, Earth Planet. Sci. Lett., 203(1), 221–233, doi:10.1016/S0012-821X(02)00848-8, 2002.

Fofonoff, N. P.: The Physical properties of seawater, in The Sea, vol. 1, edited by M. N. Hill, pp. 3–30, Interscience, New York., 1962.

Fofonoff, N. P. and Millard, R. C.: Algorithms for computation of fundamental properties of seawater, Working Paper, UNESCO, available at: https://darchive.mblwhoilibrary.org/handle/1912/2470 (Accessed 13 May 2013), 1983.

Fortuin, A. R. and Krijgsman, W.: The Messinian of the Nijar Basin (SE Spain): sedimentation, depositional environments and paleogeographic evolution, Sediment. Geol., 160(1–3), 213–242, doi:10.1016/S0037-0738(02)00377-9, 2003.

Garcia-Castellanos, D. and Villaseñor, A.: Messinian salinity crisis regulated by competing tectonics and erosion at the Gibraltar arc, Nature, 480(7377), 359–363, doi:10.1038/nature10651, 2011.

García-Lafuente, J., Sánchez-Román, A., Naranjo, C. and Sánchez-Garrido, J. C.: The very first transformation of the Mediterranean outflow in the Strait of Gibraltar, J. Geophys. Res., 116, 7 PP., doi:201110.1029/2011JC006967, 2011.

Gent, P. R. and Mcwilliams, J. C.: Isopycnal Mixing in Ocean Circulation Models, J. Phys. Oceanogr., 20(1), 150–155, doi:10.1175/1520-0485(1990)020<0150:IMIOCM>2.0.CO;2, 1990.

Gladstone, R., Flecker, R., Valdes, P., Lunt, D. and Markwick, P.: The Mediterranean hydrologic budget from a Late Miocene global climate simulation, Palaeogeogr. Palaeoclimatol. Palaeoecol., 251(2), 254–267, doi:10.1016/j.palaeo.2007.03.050, 2007.

Gordon, C., Cooper, C., Senior, C. A., Banks, H., Gregory, J. M., Johns, T. C., Mitchell, J. F. B. and Wood, R. A.: The simulation of SST, sea ice extents and ocean heat transports in a version of the Hadley Centre coupled model without flux adjustments, Clim. Dyn., 16(2), 147–168, doi:10.1007/s003820050010, 2000.

Gregory, D., Kershaw, R. and Inness, P. M.: Parametrization of momentum transport by convection. II: Tests in single-column and general circulation models, Q. J. R. Meteorol. Soc., 123(541), 1153–1183, doi:10.1002/qj.49712354103, 1997.

Griffies, S. M., Böning, C., Bryan, F. O., Chassignet, E. P., Gerdes, R., Hasumi, H., Hirst, A., Treguier, A.-M. and Webb, D.: Developments in ocean climate modelling, Ocean Model., 2(3–4), 123–192, doi:10.1016/S1463-5003(00)00014-7, 2000.

Griffin, D. L.: The late Miocene climate of northeastern Africa: unravelling the signals in the sedimentary succession, J. Geol. Soc., 156(4), 817–826, doi:10.1144/gsjgs.156.4.0817, 1999.

Haywood, A. M., Dowsett, H. J., Otto-Bliesner, B., Chandler, M. A., Dolan, A. M., Hill, D. J., Lunt, D. J., Robinson, M. M., Rosenbloom, N., Salzmann, U. and Sohl, L. E.: Pliocene Model Intercomparison Project (PlioMIP): experimental design and boundary conditions (Experiment 1), Geosci. Model Dev., 3(1), 227–242, doi:10.5194/gmd-3-227-2010, 2010.

Haywood, A. M., Ridgwell, A., Lunt, D. J., Hill, D. J., Pound, M. J., Dowsett, H. J., Dolan, A. M., Francis, J. E. and Williams, M.: Are there pre-Quaternary geological analogues for a future greenhouse warming?, Philos. Trans. R. Soc. Math. Phys. Eng. Sci., 369(1938), 933 – 956, doi:10.1098/rsta.2010.0317, 2011.

Haywood, A. M. and Valdes, P. J.: Modelling Pliocene warmth: contribution of atmosphere, oceans and cryosphere, Earth Planet. Sci. Lett., 218(3-4), 363–377, doi:16/S0012-821X(03)00685-X, 2004.

Herold, N., Huber, M., Müller, R. D. and Seton, M.: Modeling the Miocene climatic optimum: Ocean circulation, Paleoceanography, 27(1), PA1209, doi:10.1029/2010PA002041, 2012.

Hibler, W. D.: A Dynamic Thermodynamic Sea Ice Model, J. Phys. Oceanogr., 9(4), 815–846, doi:10.1175/1520-0485(1979)009<0815:ADTSIM>2.0.CO;2, 1979.

Hilgen, F. ., Bissoli, L., Iaccarino, S., Krijgsman, W., Meijer, R., Negri, A. and Villa, G.: Integrated stratigraphy and astrochronology of the Messinian GSSP at Oued Akrech (Atlantic Morocco), Earth Planet. Sci. Lett., 182(3–4), 237–251, doi:10.1016/S0012-821X(00)00247-8, 2000.

Hodell, D. A., Benson, R. H., Kent, D. V., Boersma, A. and Bied, K. R.-E.: Magnetostratigraphic, biostratigraphic, and stable isotope stratigraphy of an Upper Miocene drill core from the Salé Briqueterie (northwestern Morocco): A high-resolution chronology for the Messinian stage, Paleoceanography, 9(6), PP. 835–855, doi:199410.1029/94PA01838, 1994.

Hsu, K. J., Montadert, L., Bernoulli, D., Cita, M. B., Erickson, A., Garrison, R. E., Kidd, R. B., Mèlierés, F., Müller, C. and Wright, R.: History of the Mediterranean salinity crisis, Nature, 267(5610), 399–403, doi:10.1038/267399a0, 1977.

Hsu, K. J., Ryan, W. B. F. and Cita, M. B.: Late Miocene Desiccation of the Mediterranean, Nature, 242(5395), 240–244, doi:10.1038/242240a0, 1973.

Hüsing, S. K., Oms, O., Agustí, J., Garcés, M., Kouwenhoven, T. J., Krijgsman, W. and Zachariasse, W.-J.: On the late Miocene closure of the Mediterranean–Atlantic gateway through the Guadix basin (southern Spain), Palaeogeogr. Palaeoclimatol. Palaeoecol., 291(3–4), 167–179, doi:10.1016/j.palaeo.2010.02.005, 2010.

Ivanovic, R. F., Flecker, R., Gutjahr, M. and Valdes, P. J.: First Nd isotope record of Mediterranean–Atlantic water exchange through the Moroccan Rifian Corridor during the Messinian Salinity Crisis, Earth Planet. Sci. Lett., 368, 163–174, doi:10.1016/j.epsl.2013.03.010, 2013a.

Ivanovic, R. F., Valdes, P. J., Flecker, R., Gregoire, L. J. and Gutjahr, M.: The parameterisation of Mediterranean–Atlantic water exchange in the Hadley Centre model HadCM3, and its effect on modelled North Atlantic climate, Ocean Model., 62, 11–16, doi:10.1016/j.ocemod.2012.11.002, 2013b.

Ivanovic, R. F., Valdes, P. J., Gregoire, L., Flecker, R. and Gutjahr, M.: Sensitivity of modern climate to the presence, strength and salinity of Mediterranean-Atlantic exchange in a global general circulation model, Clim. Dyn., 1–19, doi:10.1007/s00382-013-1680-5, in press, 2013c.

Johns, T. C., Carnell, R. E., Crossley, J. F., Gregory, J. M., Mitchell, J. F. B., Senior, C. A., Tett, S. F. B. and Wood, R. A.: The second Hadley Centre coupled ocean-atmosphere GCM: model description, spinup and validation, Clim. Dyn., 13(2), 103–134, doi:10.1007/s003820050155, 1997.

Kageyama, M., Merkel, U., Otto-Bliesner, B., Prange, M., Abe-Ouchi, A., Lohmann, G., Roche, D. M., Singarayer, J., Swingedouw, D. and Zhang, X.: Climatic impacts of fresh water hosing under Last Glacial Maximum conditions: a multi-model study, Clim. Past, 9, 935-953, doi:10.5194/cp-9-935-2013, 2013.

Kahana, R.: Modelling the interactions between the Mediterranean and the Global Thermohaline Circulations, PhD thesis, University of East Anglia, Norwich, UK., 2005.

Krijgsman, W.: Astrochronology for the Messinian Sorbas basin (SE Spain) and orbital (precessional) forcing for evaporite cyclicity, Sediment. Geol., 140(1-2), 43–60, doi:10.1016/S0037-0738(00)00171-8, 2001.

Krijgsman, W., Gaboardi, S., Hilgen, F. j., Iaccarino, S., Kaenel, E. de and Laan, E. van der: Revised astrochronology for the Ain el Beida section (Atlantic Morocco): No glacio-eustatic control for the onset of the Messinian Salinity Crisis, Stratigraphy, 1, 87–101, 2004.

Krijgsman, W., Hilgen, F. J., Raffi, I., Sierro, F. J. and Wilson, D. S.: Chronology, causes and progression of the Messinian salinity crisis, Nature, 400(6745), 652–655, doi:10.1038/23231, 1999a.

Krijgsman, W., Langereis, C. G., Zachariasse, W. J., Boccaletti, M., Moratti, G., Gelati, R., Iaccarino, S. M., Papani, G. and Villa, G.: Late Neogene evolution of the Taza-Guercif Basin (Rifian Corridor, Morocco) and implications for the Messinian salinity crisis, Mar. Geol., 153(1), 147–160, doi:10.1016/S0025-3227(98)00084-X, 1999b.

Formatted: Font: (Default) Times New Roman, 12 pt

Krijgsman, W. and Meijer, P. T.: Depositional environments of the Mediterranean “Lower Evaporites” of the Messinian salinity crisis: Constraints from quantitative analyses, Mar. Geol., 253(3–4), 73–81, doi:10.1016/j.margeo.2008.04.010, 2008.

Van der Laan, E., Snel, E., Kaenel, E. de, Hilgen, F. J. and Krijgsman, W.: No major deglaciation across the Miocene-Pliocene boundary: Integrated stratigraphy and astronomical tuning of the Loulja sections (Bou Regreg area, NW Morocco), Paleoceanography, 21, 27 PP., doi:200610.1029/2005PA001193, 2006.

Lofi, J., Déverchère, J., Gaullier, V., Gillet, H., Gorini, C., Guennoc, P., Loncke, L., Maillard, A., Sage, F. and Thinon, I.: Seismic Atlas of the “Messinian Salinity Crisis” Markers in the Mediterranean and Black Seas, Commission for the Geological Map of the World, Paris, France, 2011.

Lugli, S., Manzi, V., Roveri, M. and Charlotte, S. B.: The Primary Lower Gypsum in the Mediterranean: A new facies interpretation for the first stage of the Messinian salinity crisis, Palaeogeogr. Palaeoclimatol. Palaeoecol., 297(1), 83–99, doi:10.1016/j.palaeo.2010.07.017, 2010.

Lunt, D. J., Valdes, P. J., Haywood, A. and Rutt, I. C.: Closure of the Panama Seaway during the Pliocene: implications for climate and Northern Hemisphere glaciation, Clim. Dyn., 30(1), 1–18, doi:10.1007/s00382-007-0265-6, 2008.

Markwick, P. J.: The Palaeogeographic and Palaeoclimatic Significance of Climate Proxies for Data-Model Comparisons, in Deep-Time Perspectives on Climate Change: Marrying the Signal from Computer Models and Biological Proxies (ed.s Williams, M., Haywood, A.M., Gregory, F.J. and Schmidt, D.N.), pp. 251–312, The Micropalaeontological Society Special Publications, The Geological Society, London., 2007.

Martín, J. M., Braga, J. C., Aguirre, J. and Puga-Bernabéu, Á.: History and evolution of the North-Betic Strait (Prebetic Zone, Betic Cordillera): A narrow, early Tortonian, tidal-dominated, Atlantic–Mediterranean marine passage, Sediment. Geol., 216(3–4), 80–90, doi:10.1016/j.sedgeo.2009.01.005, 2009.

Meijer, P. T.: A box model of the blocked-outflow scenario for the Messinian Salinity Crisis, Earth Planet. Sci. Lett., 248(1-2), 486–494, doi:10.1016/j.epsl.2006.06.013, 2006.

Meijer, P. T.: Hydraulic theory of sea straits applied to the onset of the Messinian Salinity Crisis, Mar. Geol., 326–328, 131–139, doi:10.1016/j.margeo.2012.09.001, 2012.

Meijer, P. T. and Krijgsman, W.: A quantitative analysis of the desiccation and re-filling of the Mediterranean during the Messinian Salinity Crisis, Earth Planet. Sci. Lett., 240(2), 510–520, doi:10.1016/j.epsl.2005.09.029, 2005.

Molnar, P.: Closing of the Central American Seaway and the Ice Age: A critical review, Paleoceanography, 23(2), PA2201, doi:10.1029/2007PA001574, 2008.

Muiños, S. B., Frank, M., Maden, C., Hein, J. R., Flierdt, T. van de, Lebreiro, S. M., Gaspar, L., Monteiro, J. H. and Halliday, A. N.: New constraints on the Pb and Nd isotopic evolution of NE Atlantic water masses, Geochem. Geophys. Geosystems, 9, 18 PP., doi:2008 10.1029/2007GC001766 [Citation], 2008.

Murdock, T. Q., Weaver, A. J. and Fanning, A. F.: Paleoclimatic response of the closing of the Isthmus of Panama in a coupled ocean-atmosphere model, Geophys. Res. Lett., 24(3), 253–256, doi:10.1029/96GL03950, 1997.

Murphy, L. N., Kirk-Davidoff, D. B., Mahowald, N. and Otto-Bliesner, B. L.: A numerical study of the climate response to lowered Mediterranean Sea level during the Messinian Salinity Crisis, Palaeogeogr. Palaeoclimatol. Palaeoecol., 279(1–2), 41–59, doi:10.1016/j.palaeo.2009.04.016, 2009.

Osborne, A. H., Frank, M. and Tiedemann, R.: The Pliocene closure of the Central American Seaway: reconstructing surface-, intermediate- and deep-water connections, oral presentation at the 22nd Goldschmidt Geochemistry Conference, Montreal (Canada), 24–29 June, 2012.

Pagani, M., Freeman, K. H. and Arthur, M. A.: Late Miocene Atmospheric CO2 Concentrations and the Expansion of C4 Grasses, Science, 285(5429), 876–879, doi:10.1126/science.285.5429.876, 1999.

Penaud, A., Eynaud, F., Sánchez-Goñi, M., Malaizé, B., Turon, J. L. and Rossignol, L.: Contrasting sea-surface responses between the western Mediterranean Sea and eastern subtropical latitudes of the North Atlantic during abrupt climatic events of MIS 3, Mar. Micropaleontol., 80(1-2), 1–17, doi:10.1016/j.marmicro.2011.03.002, 2011.

Pope, V. D., Gallani, M. L., Rowntree, P. R. and Stratton, R. A.: The impact of new physical parametrizations in the Hadley Centre climate model: HadAM3, Clim. Dyn., 16(2), 123–146, doi:10.1007/s003820050009, 2000.

Pound, M. J., Haywood, A. M., Salzmann, U. and Riding, J. B.: Global vegetation dynamics and latitudinal temperature gradients during the Mid to Late Miocene (15.97–5.33 Ma), Earth-Sci. Rev., 112(1–2), 1–22, doi:10.1016/j.earscirev.2012.02.005, 2012.

Prange, M. and Schulz, M.: A coastal upwelling seesaw in the Atlantic Ocean as a result of the closure of the Central American Seaway, Geophys. Res. Lett., 31(17), L17207, doi:10.1029/2004GL020073, 2004.

Rahmstorf, S.: Influence of Mediterranean Outflow on climate, Eos, 79(24), 281, doi:199810.1029/98EO00208, 1998.

Robinson, M. M., Valdes, P. J., Haywood, A. M., Dowsett, H. J., Hill, D. J. and Jones, S. M.: Bathymetric controls on Pliocene North Atlantic and Arctic sea surface temperature and deepwater production, Palaeogeogr. Palaeoclimatol. Palaeoecol., 309(1-2), 92–97, doi:16/j.palaeo.2011.01.004, 2011.

Rogerson, M., Colmenero-Hidalgo, E., Levine, R. C., Rohling, E. J., Voelker, A. H. L., Bigg, G. R., Schönfeld, J., Cacho, I., Sierro, F. J., Löwemark, L., Reguera, M. I., Abreu, L. de and Garrick, K.: Enhanced Mediterranean-Atlantic exchange during Atlantic freshening phases, Geochem. Geophys. Geosystems, 11, 22 PP., doi:201010.1029/2009GC002931, 2010.

Rogerson, M., Rohling, E. J., Bigg, G. R. and Ramirez, J.: Paleoceanography of the Atlantic-Mediterranean exchange: Overview and first quantitative assessment of climatic forcing, Rev. Geophys., 50, 32 PP., doi:201210.1029/2011RG000376, 2012.

Rogerson, M., Rohling, E. J. and Weaver, P. P. E.: Promotion of meridional overturning by Mediterranean-derived salt during the last deglaciation, Paleoceanography, 21, 8 PP., doi:200610.1029/2006PA001306, 2006.

Roveri, M., Bergamasco, A., Carniel, S., Gennari, R., Lugli, S. and Manzi, V.: The origin of Messinian canyons in the Mediterranean basin: towards an alternative model for the Messinian Salinity Crisis, oral presentation at the joint RCMNS-RCANS Interim Colloquium, Salamanca, Spain, 21–23 September, 2011.

Roveri, M., Lugli, S., Manzi, V. and Schreiber, B. C.: The Messinian Sicilian stratigraphy revisited: new insights for the Messinian salinity crisis, Terra Nova, 20(6), 483–488, doi:10.1111/j.1365-3121.2008.00842.x, 2008.

Ryan, W. B. F. and Cita, M. B.: The nature and distribution of Messinian erosional surfaces — Indicators of a several-kilometer-deep Mediterranean in the Miocene, Mar. Geol., 27(3–4), 193–230, doi:10.1016/0025-3227(78)90032-4, 1978.

Ryan, W. B. F., Hsu, K. J., Cita, M. B., Dumitrica, P., Lort, J. M., Maync, W., Nesteroff, W. D., Pautot, G., Stradner, H., and Wezel, F. C.: Initial Reports of the Deep Sea Drilling Project, 13, U.S. Government Printing Office, available at http://deepseadrilling.org/13/dsdp_toc.htm (last access: 19 June 2012), 1973.

Santisteban, C. and Taberner, C.: Shallow marine and continental conglomerates derived from coral reef complexes after desiccation of a deep marine basin: the Tortonian-Messinian deposits of the Fortuna Basin, SE Spain, J. Geol. Soc., 140(3), 401–411, doi:10.1144/gsjgs.140.3.0401, 1983.

Schneck, R., Micheels, A. and Mosbrugger, V.: Climate modelling sensitivity experiments for the Messinian Salinity Crisis, Palaeogeogr. Palaeoclimatol. Palaeoecol., 286(3-4), 149–163, doi:10.1016/j.palaeo.2009.12.011, 2010.

Schneider, B. and Schmittner, A.: Simulating the impact of the Panamanian seaway closure on ocean circulation, marine productivity and nutrient cycling, Earth Planet. Sci. Lett., 246(3-4), 367–380, doi:16/j.epsl.2006.04.028, 2006.

Simmons, A. J. and Burridge, D. M.: An Energy and Angular-Momentum Conserving Vertical Finite-Difference Scheme and Hybrid Vertical Coordinates, Mon. Weather Rev., 109(4), 758–766, doi:10.1175/1520-0493(1981)109<0758:AEAAMC>2.0.CO;2, 1981.

Steph, S., Tiedemann, R., Prange, M., Groeneveld, J., Schulz, M., Timmermann, A., Nürnberg, D., Rühlemann, C., Saukel, C. and Haug, G. H.: Early Pliocene increase in thermohaline overturning: A precondition for the development of the modern equatorial Pacific cold tongue, Paleoceanography, 25(2), PA2202, doi:10.1029/2008PA001645, 2010.

Stouffer, R. J., Yin, J., Gregory, J. M., Dixon, K. W., Spelman, M. J., Hurlin, W., Weaver, A. J., Eby, M., Flato, G. M., Hasumi, H., Hu, A., Jungclaus, J. H., Kamenkovich, I. V., Levermann, A., Montoya, M., Murakami, S., Nawrath, S., Oka, A., Peltier, W. R., Robitaille, D. Y., Sokolov, A., Vettoretti, G. and Weber, S. L.: Investigating the Causes of the Response of the Thermohaline Circulation to Past and Future Climate Changes, J. Clim., 19(8), 1365–1387, doi:10.1175/JCLI3689.1, 2006.

Thierstein, H. R. and Berger, W. H.: Injection events in ocean history, Nature, 276(5687), 461–466, doi:10.1038/276461a0, 1978.

Topper, R. P. M., Flecker, R., Meijer, P. T. and Wortel, M. J. R.: A box model of the Late Miocene Mediterranean Sea: Implications from combined 87Sr/86Sr and salinity data, Paleoceanography, 26(3), PA3223, doi:10.1029/2010PA002063, 2011.

Visbeck, M., Marshall, J., Haine, T. and Spall, M.: Specification of Eddy Transfer Coefficients in Coarse-Resolution Ocean Circulation Models*, J. Phys. Oceanogr., 27(3), 381–402, doi:10.1175/1520-0485(1997)027<0381:SOETCI>2.0.CO;2, 1997.

Voelker, A. H. L., Lebreiro, S., Schonfeld, J., Cacho, I., Erlenkeuser, H. and Abrantes, F.: Mediterranean outflow strengthening during northern hemisphere coolings: A salt source for the glacial Atlantic?, Earth Planet. Sci. Lett., 245(1-2), 39–55, doi:10.1016/j.epsl.2006.03.014, 2006.

Van de Wal, R. S. W., de Boer, B., Lourens, L. J., Köhler, P. and Bintanja, R.: Reconstruction of a continuous high-resolution CO2 record over the past 20 million years, Clim Past, 7(4), 1459–1469, doi:10.5194/cp-7-1459-2011, 2011.

Wu, W., Danabasoglu, G. and Large, W. G.: On the effects of parameterized Mediterranean overflow on North Atlantic ocean circulation and climate, Ocean Model., 19(1–2), 31–52, doi:10.1016/j.ocemod.2007.06.003, 2007.

Zhang, R. and Delworth, T. L.: Simulated Tropical Response to a Substantial Weakening of the Atlantic Thermohaline Circulation, J. Clim., 18(12), 1853–1860, doi:10.1175/JCLI3460.1, 2005.

Zhang, X., Prange, M., Steph, S., Butzin, M., Krebs, U., Lunt, D. J., Nisancioglu, K. H., Park, W., Schmittner, A., Schneider, B. and Schulz, M.: Changes in equatorial Pacific thermocline depth in response to Panamanian seaway closure: Insights from a multi-model study, Earth Planet. Sci. Lett., 317–318, 76–84, doi:10.1016/j.epsl.2011.11.028, 2012.

Table 1. Summary of the differences between all simulations. For *Messinian control* and *no-exchange*, Mediterranean salinity was left unforced, resulting in normal, open marine salinity conditions of ~44 psu for the basin.

Experiment name	Mediterranean outflow	Mediterranean salinity	Coefficient of exchange (μ)	Mediterranean salt export to Atlantic
control	present	unforced	μ_C	1.2 psu Sv
no-exchange	blocked	unforced	no exchange	0
halite-quarter	present	380 psu	$0.25\mu_C$	20.6 psu Sv
halite-normal[a]	present	380 psu	μ_C	84.2 psu Sv
gypsum-half	present	130 psu	$0.5\mu_C$	11.0 psu Sv
gypsum-normal[a]	present	130 psu	μ_C	22.4 psu Sv
fresh-half[a]	present	5 psu	$0.5\mu_C$	-3.0 psu Sv
fresh-normal	present	5 psu	μ_C	-7.0 psu Sv
fresh-double[a]	present	5 psu	$2\mu_C$	-14.2 psu Sv

[a] Simulations not discussed explicitly in the text.

~~Experiment name~~	~~Mediterranean Outflow Water~~	~~Mediterranean salinity~~	~~Coefficient of exchange (μ)~~
~~*control*~~	~~present~~	~~unforced~~	~~μ_c~~
~~*no-exchange*~~	~~blocked~~	~~unforced~~	~~no exchange~~
~~*halite-quarter*~~	~~present~~	~~380 psu~~	~~$0.25\mu_c$~~
~~*halite-normal**~~	~~present~~	~~380 psu~~	~~μ_c~~
~~*gypsum-half*~~	~~present~~	~~130 psu~~	~~$0.5\mu_c$~~
~~*gypsum-normal**~~	~~present~~	~~130 psu~~	~~μ_c~~
~~*fresh-half**~~	~~present~~	~~5 psu~~	~~$0.5\mu_c$~~
~~*fresh-normal*~~	~~present~~	~~5 psu~~	~~μ_c~~
~~*fresh-double**~~	~~present~~	~~5 psu~~	~~$2\mu_c$~~

~~*Simulations not discussed explicitly in the text.~~

Formatted: Font: Not Italic

Formatted: Font: Not Italic

Formatted: Font: Not Italic

Formatted: Font: Not Italic, Superscript

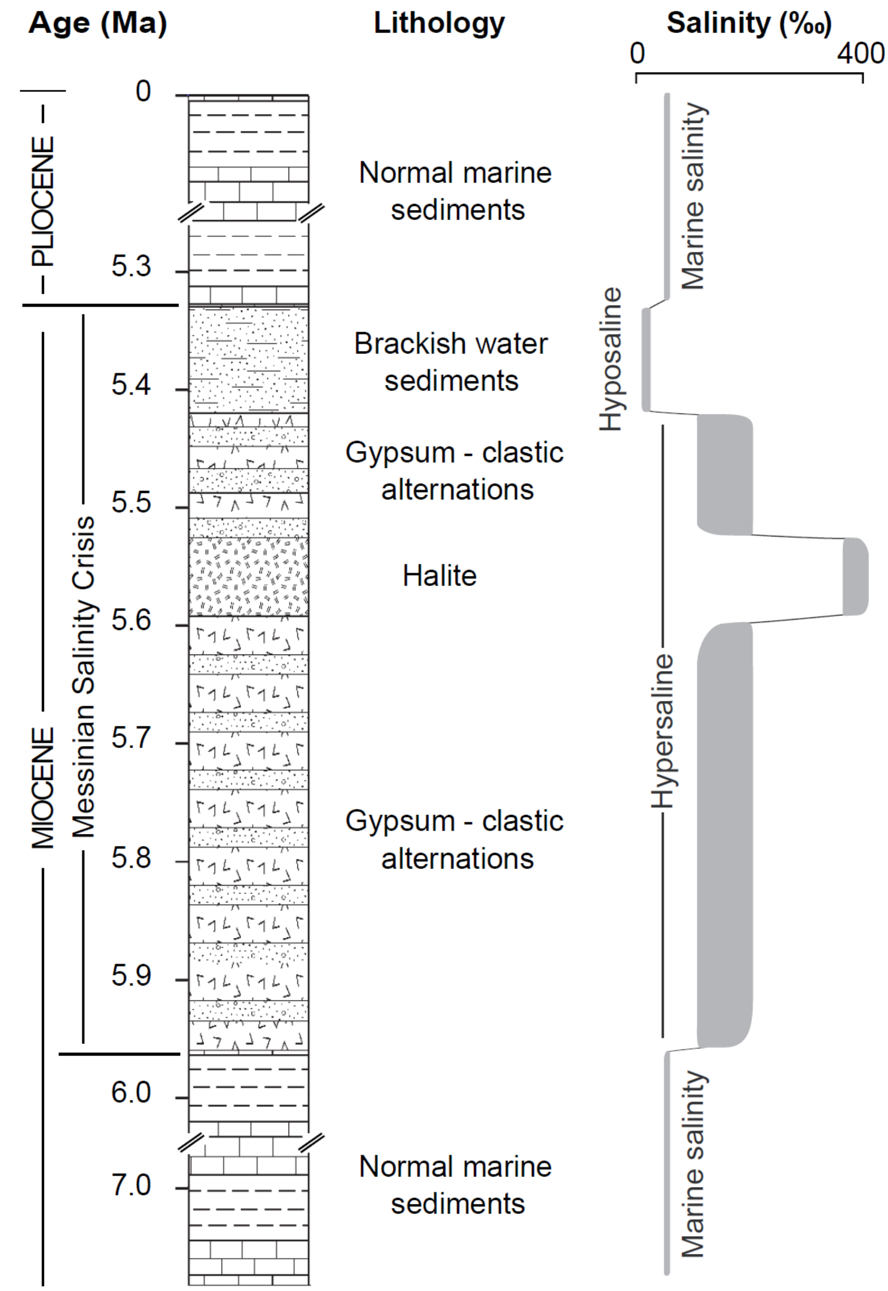

Figure 1. Schematic composite section of the main Mediterranean lithologies over the Messinian Salinity Crisis, including the corresponding salinities in which the successions were deposited/precipitated (after Ivanovic et al., 2013a). Timing of event boundaries are after Roveri et al. (2008) and references therein.

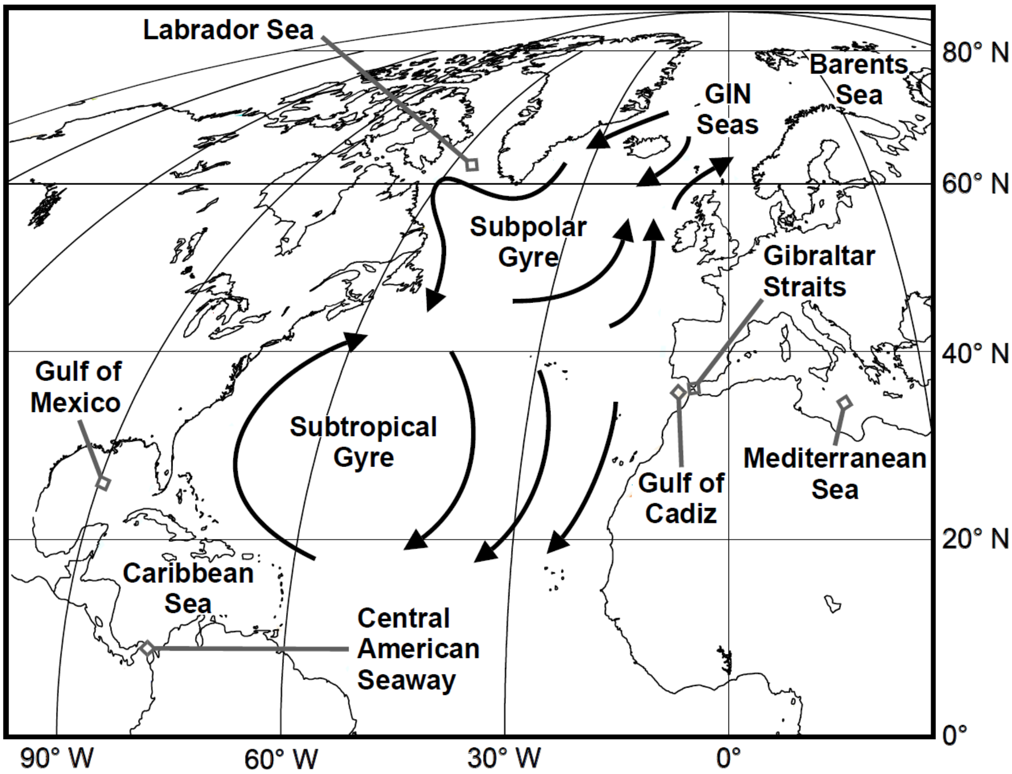

Figure 2. Map of the North Atlantic region marked with key geographical areas discussed in the text. Schematic representations of the modern North Atlantic subtropical and subpolar ocean gyre circulations are also shown.

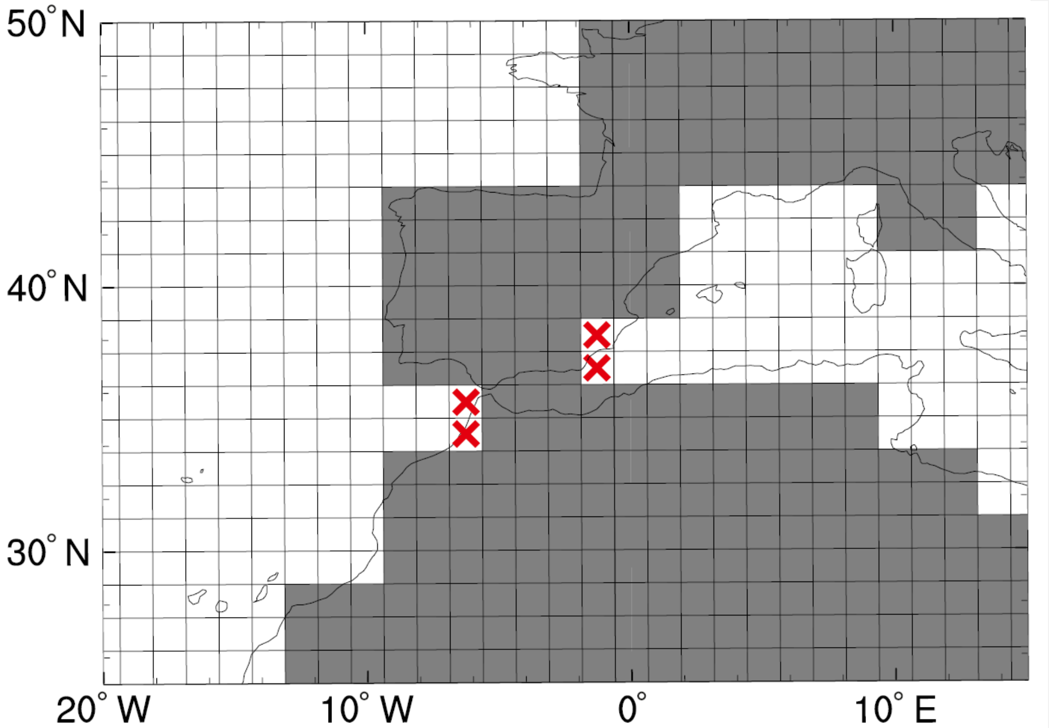

Fig. 3. HadCM3 land-sea mask in the Gibraltar Straits region, with the model's ocean grid and modern coastline overlain. Land is in grey, ocean in white. The four red crosses mark the grid boxes either side of the European-African land-bridge that are connected by the 'pipe' parameterisation of Mediterranean-Atlantic water exchange (see text in Sect. 2.2).

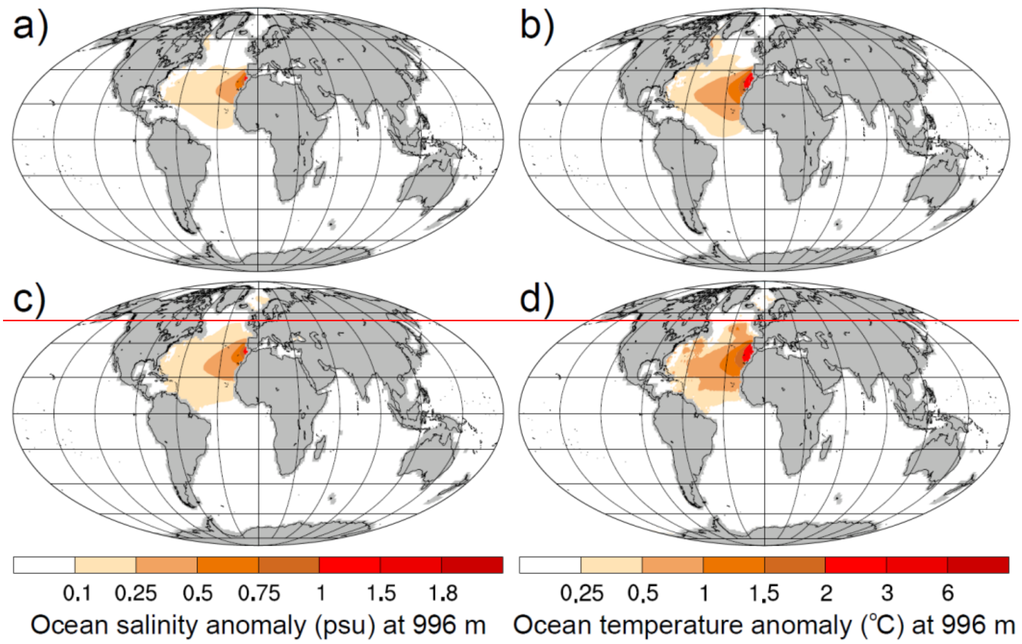

~~Figure 3. Annual mean difference between a simulation with MOW versus a simulation without MOW for (a, c) ocean salinity (in psu) and (b, d) ocean potential temperature (in °C) both at a depth of 996 m, for a modern (pre-industrial) control simulation (top: a, b) (Ivanovic et al., in press) and a Messinian simulation (bottom: c, d). Continental landmasses are masked in grey. Note that for orientation, a modern coastal outline is shown, latitude parallels are 20° apart and longitude parallels are 30° apart. Figures 4, 6, 8 and 9 also use this projection.~~

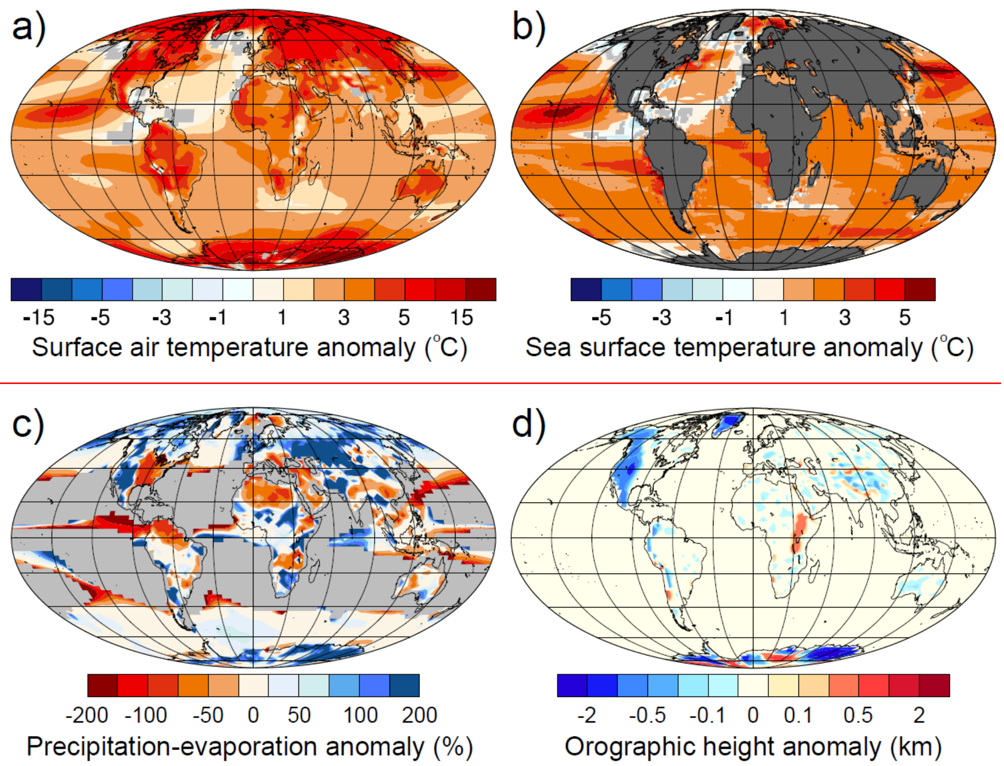
a)
-15 -5 -3 -1 1 3 5 15
Surface air temperature anomaly (°C)
b)
-5 -3 -1 1 3 5
Sea surface temperature anomaly (°C)
c)
-200 -100 -50 0 50 100 200
Precipitation-evaporation anomaly (%)
d)
-2 -0.5 -0.1 0 0.1 0.5 2
Orographic height anomaly (km)

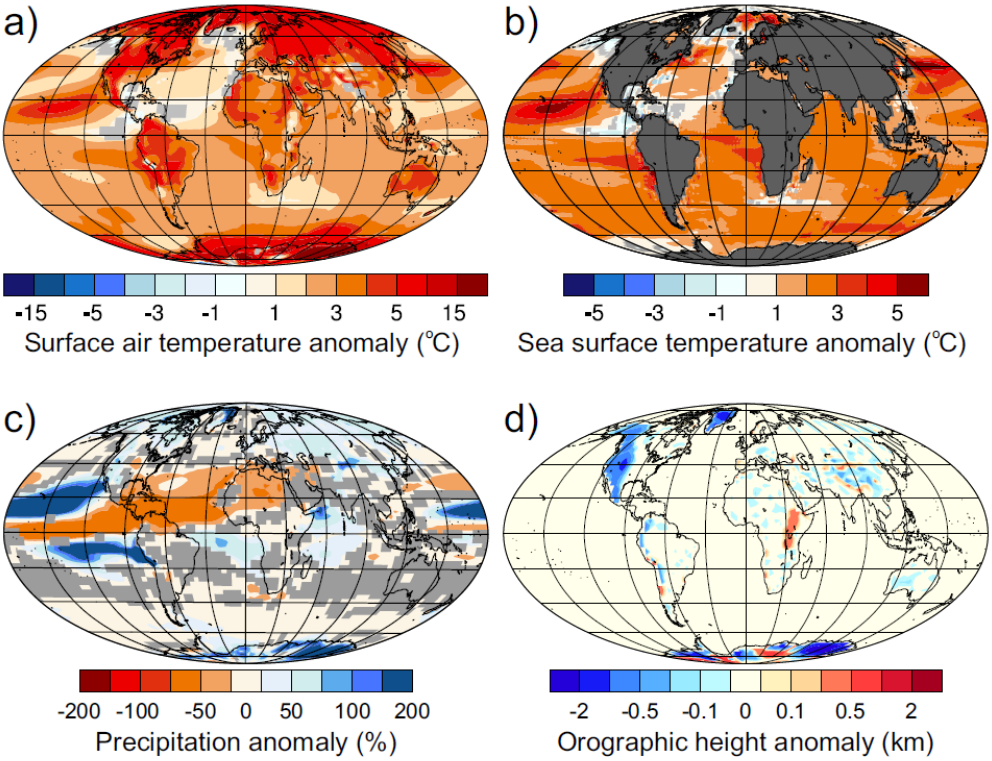

Figure ~~4~~4. Annual mean difference between the *Messinian control* versus the modern (pre-industrial) *control* simulation (as used by Ivanovic et al., ~~in press~~2013c) for (a) surface air temperature (in °C), (b) sea surface temperature (in °C), (c) precipitation~~ minus evaporation~~ (%), and (d) surface orography (in km). Anomalies with <95% confidence in significance using a student *t*-test are masked in light grey. For orientation, a modern coastal outline is shown, latitude parallels are 20° apart and longitude parallels are 30° apart. Figure 10 also uses this projection.

Formatted: Font: Italic

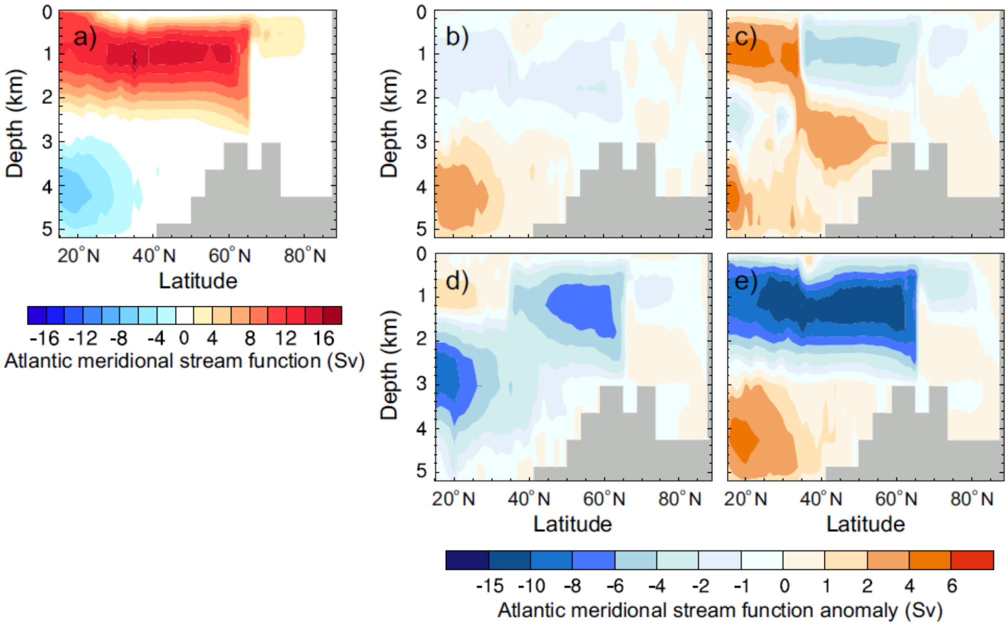

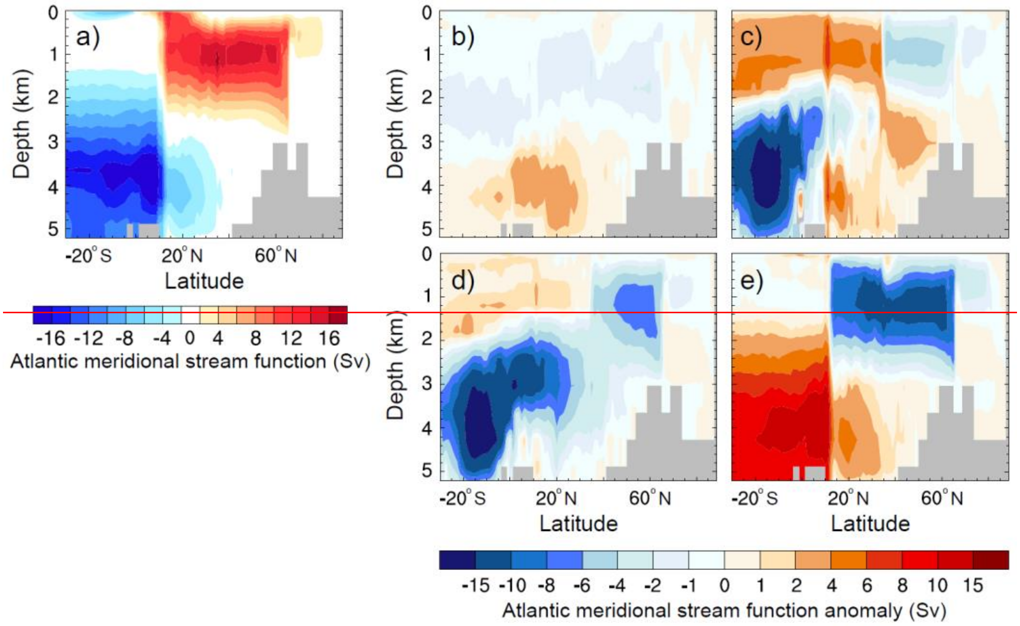

Figure ~~5~~5. Atlantic Meridional Overturning Circulation (AMOC) stream function (in Sv) for (a) *Messinian control*; and AMOC stream function anomalies, given with respect to *Messinian control*, for (b) *no-exchange*, (c) *halite-quarter*, (d) *gypsum-half* and (e) *fresh-normal*. Positive (negative) stream function indicates strength in the clockwise (counter-clockwise) direction. Note that because of the open Central American Seaway in the Miocene, the Atlantic basin is only enclosed north of 15° N; hence the stream function is plotted from 15° N to 90° N. Bathymetry is masked in grey.

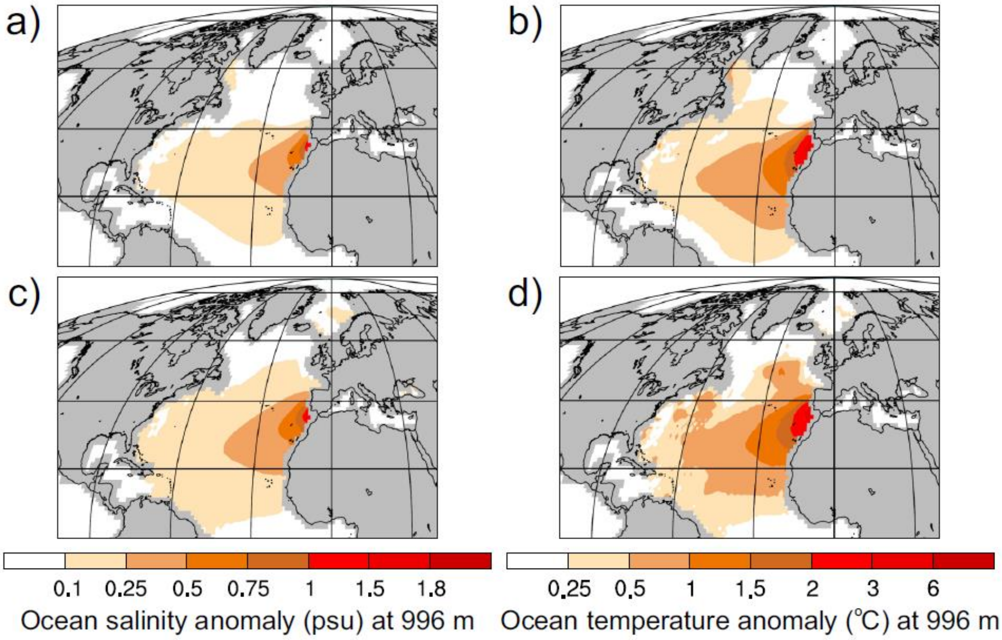

Figure 6. North Atlantic annual mean difference between a simulation with MOW versus a simulation without MOW for (a, c) ocean salinity (in psu) and (b, d) ocean potential temperature (in °C) both at a depth of 996 m, for a modern (pre-industrial) control simulation (top: a, b) (Ivanovic et al., 2013c) and a Messinian simulation (bottom: c, d). Continental landmasses are masked in grey. Note that for orientation, a modern coastal outline is shown, latitude parallels are 20° apart and longitude parallels are 30° apart. Figures 7 and 9 also use this projection.

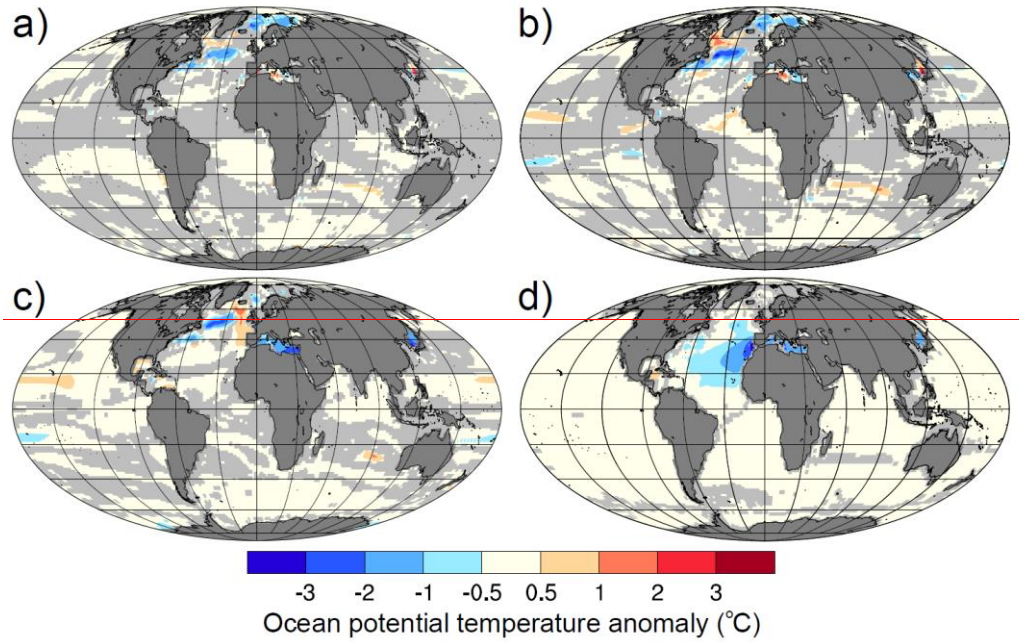

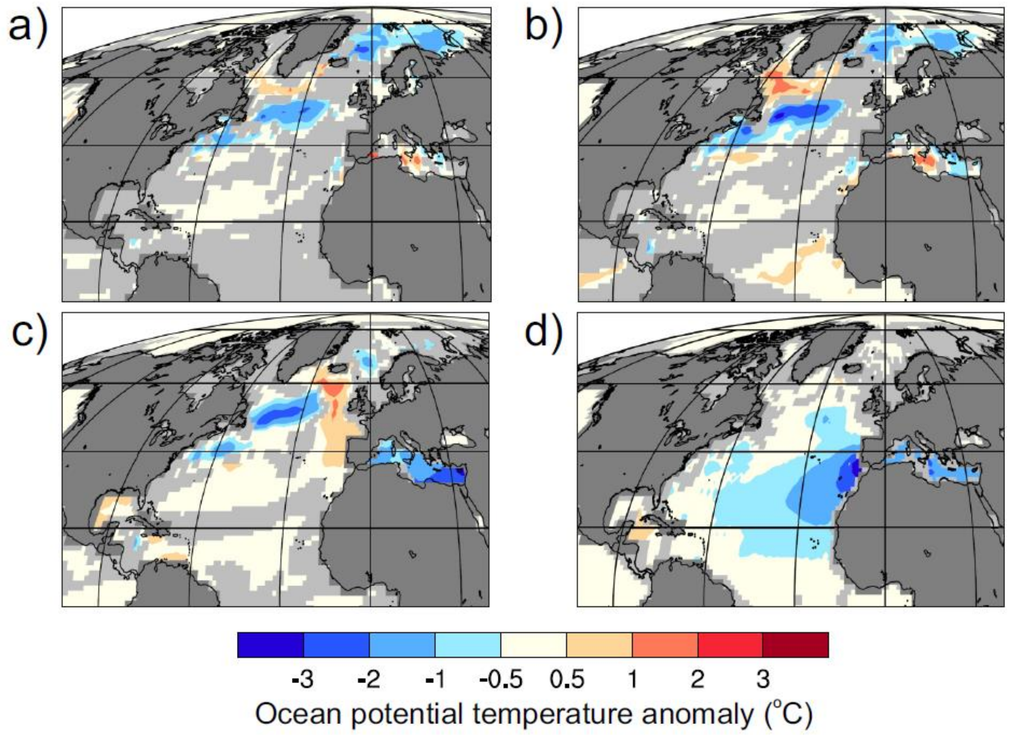

Figure ~~6~~7. North Atlantic a~~A~~nnual mean ocean potential temperature anomalies (in °C) for *no-exchange* with respect to *Messinian control* at a depth of (a) 5 m (b) 67 m, (c) 301 m and

(d) 996 m. Continental land masses are masked in dark grey. Anomalies with <95 % confidence in significance using a student *t*-test are masked in light grey.

Formatted: Font: Italic

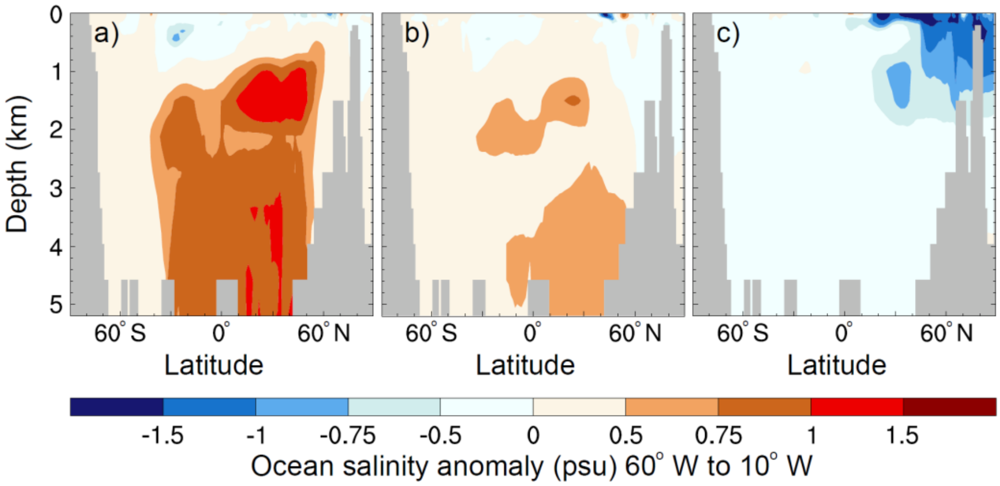

Figure ~~7~~8. Annual mean ocean salinity anomalies (in psu) from the North to South Pole, averaged over 60° W to 10° W and given with respect to *Messinian control* for (a) *halite-quarter*, (b) *gypsum-half* and (c) *fresh-normal*. Bathymetry is masked in grey. All anomalies are given with >95 % confidence in their significance using a student *t*-test.

Formatted: Font: Italic

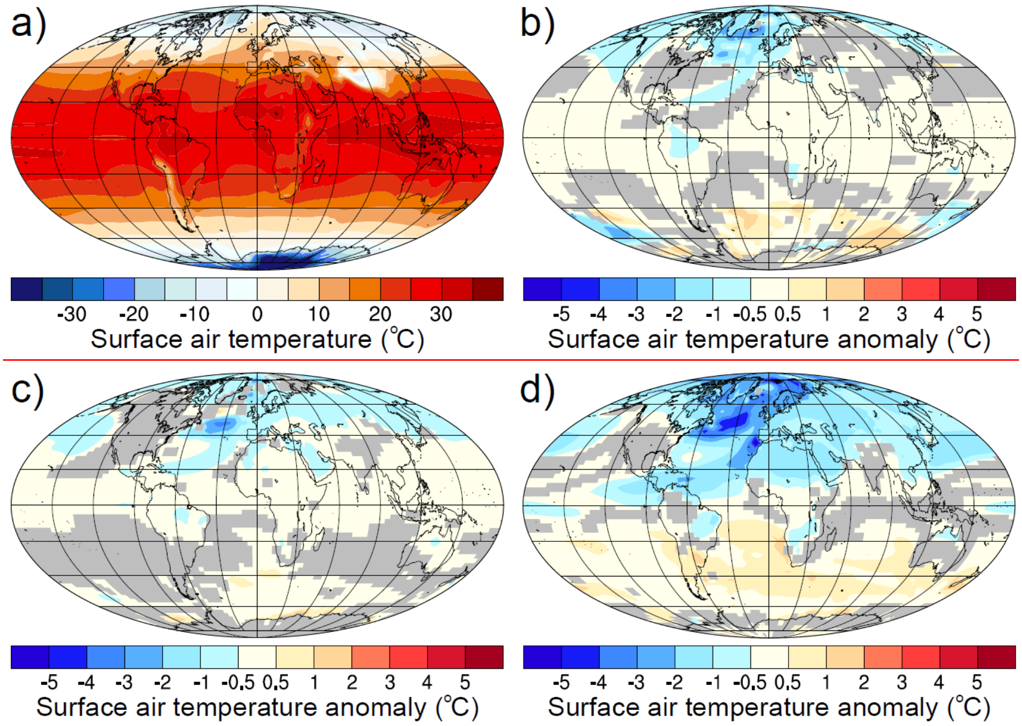
a)
b)
c)
d)
-30 -20 -10 0 10 20 30
Surface air temperature (°C)
-5 -4 -3 -2 -1 -0.5 0.5 1 2 3 4 5
Surface air temperature anomaly (°C)

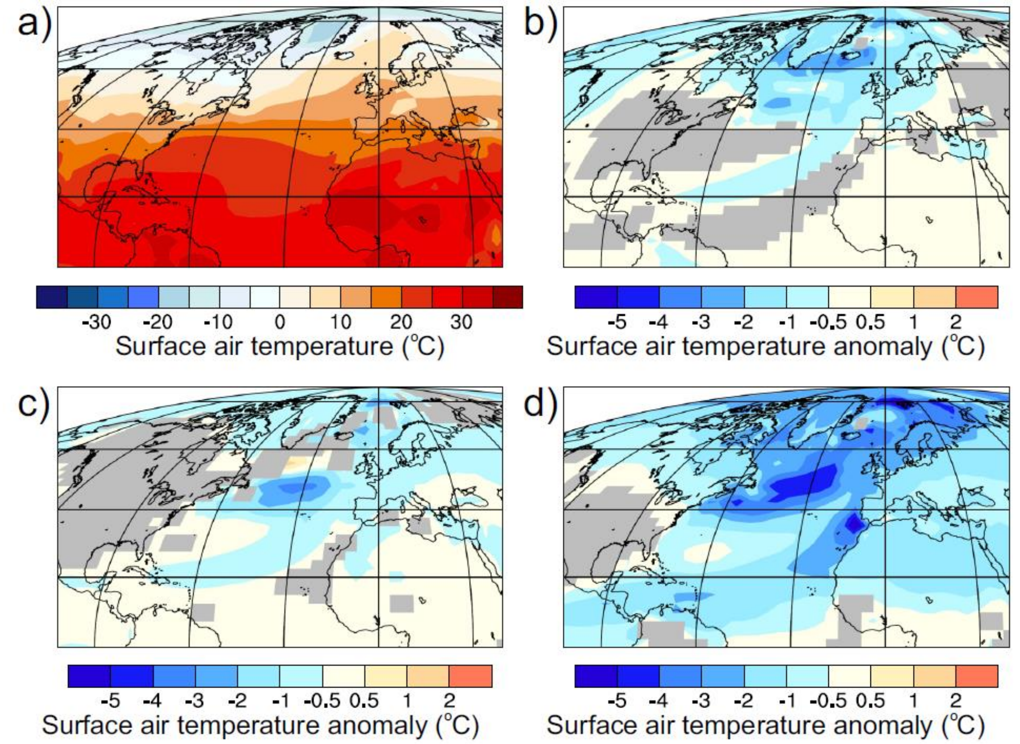
a)
b)
c)
d)
-30 -20 -10 0 10 20 30
Surface air temperature (°C)
-5 -4 -3 -2 -1 -0.5 0.5 1 2
Surface air temperature anomaly (°C)

Figure ~~8~~9. North Atlantic a~~A~~nnual mean surface air temperatures (in °C) for (a) *Messinian control* and annual mean surface air temperature anomalies, given with respect to *Messinian control*, for (b) *halite-quarter*, (c) *gypsum-half* and (d) *fresh-normal*. The magnitudes of some of the local anomalies are difficult to identify, especially in the high latitudes, but numbers quoted in the text are accurate. Anomalies with <95 % confidence in significance using a student ~~t~~*t*-test are masked in light grey.

Formatted: Font: Italic

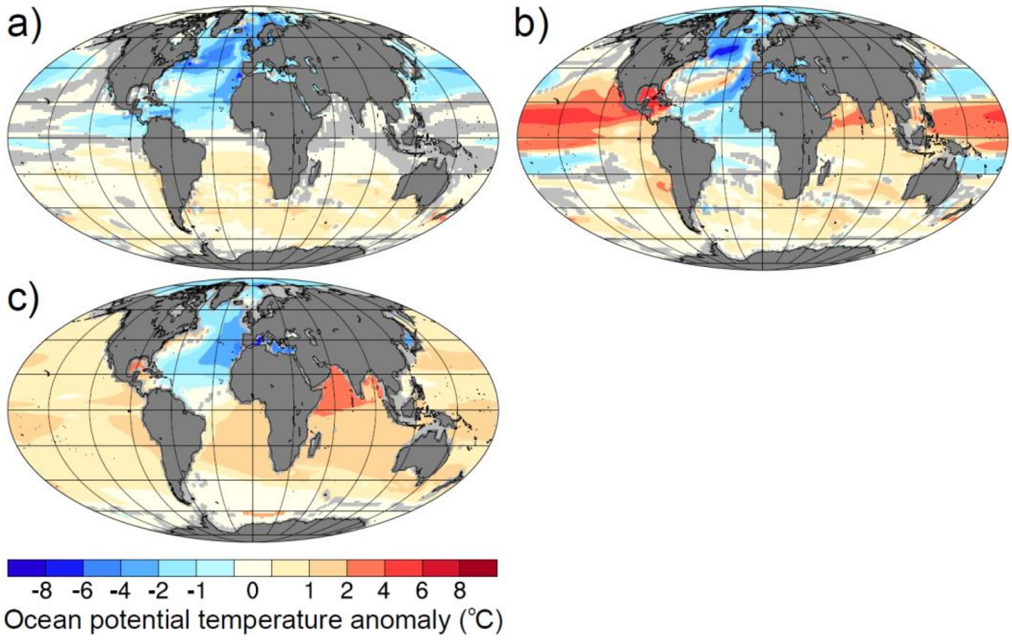

Figure ~~9~~10. Annual mean ocean potential temperature anomalies (in °C) for *fresh-normal* with respect to *Messinian control* at a depth of (a) 5 m (b) 204 m and (c) 996 m. Continental land masses are masked in dark grey. Anomalies with <95 % confidence in significance using a student *t*-test are masked in light grey.

Formatted: Font: Italic